ΕΛΛΗΝΙΚΗ ΔΗΜΟΚΡΑΤΙΑ
ΠΑΝΕΠΙΣΤΗΜΙΟ ΙΩΑΝΝΙΝΩΝ
ΠΡΟΓΡΑΜΜΑ ΜΕΤΑΠΤΥΧΙΑΚΩΝ ΣΠΟΥΔΩΝ
«ΠΡΟΗΓΜΕΝΑ ΥΛΙΚΑ»
ΤΜΗΜΑ ΜΗΧΑΝΙΚΩΝ ΕΠΙΣΤΗΜΗΣ ΥΛΙΚΩΝ
ΣΧΟΛΗ ΘΕΤΙΚΩΝ ΕΠΙΣΤΗΜΩΝ

ΜΕΤΑΠΤΥΧΙΑΚΗ ΔΙΑΤΡΙΒΗ

ΜΑΡΙΑ ΜΠΟΥΡΗ

ΤΙΤΛΟΣ ΜΕΤΑΠΤΥΧΙΑΚΗΣ ΔΙΑΤΡΙΒΗΣ

ΔΟΜΙΚΕΣ ΚΑΙ ΗΛΕΚΤΡΟΝΙΑΚΕΣ ΙΔΙΟΤΗΤΕΣ ΤΗΣ L-ΓΛΟΥΤΑΜΙΝΗΣ ΣΕ ΕΠΙΦΑΝΕΙΑ ΧΑΛΚΟΥ (111) ΜΕ ΥΠΟΛΟΓΙΣΜΟΥΣ ΠΡΩΤΩΝ ΑΡΧΩΝ

ΙΩΑΝΝΙΝΑ, ΕΤΟΣ 2015

Εσώφυλλο:

Η παρούσα Μεταπτυχιακή Διατριβή εκπονήθηκε στο πλαίσιο των σπουδών για την απόκτηση του Μεταπτυχιακού Διπλώματος Ειδίκευσης στην εξειδίκευση:

Υπολογιστική Επιστήμη και Μοντελοποίηση Υλικών

που απονέμει το Τμήμα Μηχανικών Επιστήμης Υλικών του Πανεπιστημίου Ιωαννίνων.

Εγκρίθηκε την 22/12/15 από την εξεταστική επιτροπή:

ΟΝΟΜΑΤΕΠΩΝΥΜΟ **ΒΑΘΜΙΔΑ**

1. Λέκκα Χριστίνα, Αναπλ. Καθηγήτρια

2. Παπαγεωργίου Δημήτριος, Αναπλ. Καθηγητής……..

3. Λοιδωρίκης Ελευθέριος, Αναπλ. Καθηγητής……

ΥΠΕΥΘΥΝΗ ΔΗΛΩΣΗ

"Δηλώνω υπεύθυνα ότι η παρούσα διατριβή εκπονήθηκε κάτω από τους διεθνείς ηθικούς και ακαδημαϊκούς κανόνες δεοντολογίας και προστασίας της πνευματικής ιδιοκτησίας. Σύμφωνα με τους κανόνες αυτούς, δεν έχω προβεί σε ιδιοποίηση ξένου επιστημονικού έργου και έχω πλήρως αναφέρει τις πηγές που χρησιμοποίησα στην εργασία αυτή."

Μπούρη Μαρία

(Υπογραφή υποψήφιας)

ΠΡΟΛΟΓΟΣ - Acknowledgements

The present study accomplished within the Master program “Advanced Materials” in the Department of Material Science and Engineering at the University of Ioannina.

I would like to express my sincere gratitude to my advisor Assoc. Prof. Christina Lekka for the continuous support of my Master study, for her patience, motivation, and immense knowledge. Her guidance helped me in all the time of research and writing of this thesis.

I would like to thank my parents for supporting me spiritually throughout writing this thesis and my life in general. This thesis would not have been possible without their support.

I would also like to thank the member of my committee Assoc. Prof. D. Papageorgiou and Assoc. Prof Lidorikis as well as Prof. Evangelakis for fruitful discussions and my laboratory colleges for their support and friendship.

Περίληψη

Η διάβρωση των μεταλλικών επιφανειών προκαλεί οικονομικό πλήγμα στις βιομηχανίες και μόλυνση του περιβάλλοντος. Για τη προστασία των επιφανειών από τη διάβρωση, έχουν χρησιμοποιηθεί οργανικοί, μη τοξικοί αναστολείς όπως για παράδειγμα τα αμινοξέα. Έρευνες έχουν δείξει ότι τα ελεύθερα ηλεκτρόνια των ετεροατόμων των αναστολέων ή τα π ηλεκτρόνια είναι διαθέσιμα να σχηματίσουν δεσμούς με το υπόστρωμα και να δράσουν ως πυρηνόφιλα διευκολύνοντας τη διαδικασία προσρόφησης των αναστολέων στη μεταλλική επιφάνεια. Στην παρούσα εργασία, μελετήθηκε θεωρητικά η συμπεριφορά του αμινοξέος L-γλουταμίνη ως αναστολέας διάβρωσης της επιφάνειας Χαλκού (111).

Πραγματοποιήθηκαν υπολογισμοί με τη θεωρία Συναρτησιακού Πυκνότητας Φορτίου (Density Functional Theory) μέσω του κώδικα SIESTA ώστε να ερευνηθούν οι διατάξεις της L-γλουταμίνης με την ελάχιστη ενέργεια. Ξεκινώντας από την επιφάνεια (111) του Χαλκού, η L-γλουταμίνη τοποθετήθηκε ομαλά πάνω στην επιφάνεια σε διάφορες πιθανές διατάξεις. Για την ενεργειακά προτιμητέα διάταξη εκτιμήθηκαν οι ηλεκτρονικές ιδιότητες του συστήματος ώστε να ερευνηθούν τα ενεργά κέντρα της L-γλουταμίνης. Οι υπολογισμοί απέδειξαν ότι η L-γλουταμίνη μπορεί να σχηματίσει δεσμικές καταστάσεις με τα άτομα του χαλκού μέσω των ετεροατόμων της Άζωτο και Οξυγόνο στο ενεργειακό φάσμα -3 eV to -5eV. Η ικανότητα δημιουργίας ενός συνεχούς καλύμματος πάνω στη μεταλλική επιφάνεια μελετήθηκε μέσω της επικάλυψης της επιφάνειας χαλκού (111) τοποθετώντας δύο μόρια L-γλουταμίνης. Ενεργειακά προτιμητέα διάταξη βρέθηκε η παράλληλη τοποθέτηση των μορίων σε σύγκριση με την αντί-παράλληλη διάταξη. Επίσης, παρατηρήθηκαν αλληλεπιδράσεις μεταξύ των μορίων και κατευθυντικοί υβριδισμοί με το υπόστρωμα υποδηλώνοντας τη σταθερότητα του καλύμματος. Τέλος, Προσομοίωσεις πρώτων αρχών Μοριακής Δυναμικής πραγματοποιήθηκαν σε διάφορες διατάξεις της L-γλουταμίνης πάνω στην επιφάνεια χαλκού (111) υποστηρίζοντας την οριζόντια στοίχιση. Ενδιαφέρον προκαλεί ότι η κάθετη εναπόθεση της L-γλουταμίνης στην επιφάνεια απαιτεί μόνο 1 psec, σε θερμοκρασία δωματίου ώστε να περιστραφεί παράλληλα προς το υπόστρωμα.

Τα αποτελέσματα αυτά θα μπορούσαν να χρησιμοποιηθούν για τη δημιουργία μιας ανθεκτικής ως προς τη διάβρωση επικάλυψης των επιφανειών χαλκού.

Abstract

Corrosion of metal surfaces causes financial damages to the industries and environmental pollution. For the protection of surfaces from corrosion, organic non- toxic inhibitors like amino acids have been used. Researches have shown that the inhibitor molecule's free electron pairs of heteroatoms or the π electrons are readily available to form bonds with the substrate and act therefore as nucleophile centers greatly facilitating in the adsorption processes over the metallic surface. In this thesis a theoretically study has been performed using L-glutamine amino acid as corrosion inhibitor of the Cu (111) surface.

Density Functional Theory (DFT) calculations within the SIESTA code have been used to investigate the minimum energy configurations of L-glutamine on Cu (111) surface. Starting from the Cu (111) surface, the L-glutamine was softly deposited according to several possible configurations. For the energetically favoured alignment the electronic properties were evaluated in order to investigate the active site of L-glutamine. Calculations proved that L-glutamine form bonded states with the Cu atoms through its heteroatoms Nitrogen and Oxygen at the energy range from -3 eV to -5eV. The ability of a continues coating on metallic surface was considered through the coverage of Cu (111) super cell with two L-glutamine molecules. The parallel alignment between the two molecules was found energetically favoured compared to the anti-parallel while intermolecular interactions and bonding hybridizations with the substrate were observed denoting the stability of the coating. Finally ab initio Molecular Dynamics simulations were performed on several configurations of L-glutamine on Cu (111) surface supporting the horizontal alignment. Interestingly, the vertical L-glutamine's adsorption on the surface requires only ~1 psec, at room temperature to rotate parallel to the substrate.

These results could be used for the creation of a corrosion resistant coating on Cu surfaces.

INDEX

Figure Index

Table Index

1. INTRODUCTION

1.1 METAL SURFACES

Copper reveals high electrical conductivity, ductility, and malleability, good mechanical workability, relatively low cost and reactivity. Therefore Copper is one of the most important materials used in different industries, especially in central heating installations, car industry, energy industries, oil refineries, sugar refineries, marine environment and in several technological applications [22],[21]. Although Copper develops a strongly adhering oxide layer, which thickens to acquire the familiar green patina found on copper roofs. In the presence of atmospheric sulfur dioxide (SO_2) the transition from oxide layer to patina is accelerated. In several architecture structures such as roofing, where the green patina has aesthetic value, the increase in formation of patina is desirable. This is definitely not the case in electrical system applications and microelectronic devices where the formation of this thick non-conductive patina is undesirable [33] resulting the protection of Cu surfaces from corrosion very important e.g. for the industries.

Small amounts of alloying elements are often added to metals to improve certain characteristics of the metal. Alloying can increase or reduce the strength, hardness, electrical and thermal conductivity, corrosion resistance, or change the color of a metal [35]. Due to novel properties of materials fabricated out of typically immiscible alloys, like high thermal and electrical conductivity and excellent magnetic properties (i.e. high magnetoresistance and coercivity), a long-standing interest in the preparation of such alloys exists [36].

Iron is a widely used material with extensive industrial application because of its interesting properties such as electrical conductivity, malleability, ductility etc. The stable phase of Fe is a ferromagnetic body centered cubic (bcc) lattice. At high temperatures the Fe becomes face centered cubic (fcc) and is non-magnetic [37].

Copper-iron master alloy is used as a grain refiner for some brass alloys and aluminium bronze. It is also used for improving mechanical properties of low alloyed coppers and corrosion resistance of copper-nickel alloys [38]. Due to novel properties of materials fabricated out of typically immiscible alloys, like high thermal and electrical

conductivity and excellent magnetic properties (i.e. high magnetoresistance and coercivity), a long-standing interest in the preparation of such alloys exists [36].

1.2 CORROSION OF METALLIC SURFACES AND CORROSION INHIBITORS

Valuable metals such as iron, copper and aluminum are prone to corrosion when they are exposed to aggressive medium (i.e. acids, bases, salts) leading to pollution risks and great economic impacts [1]. Corrosion processes develop fast after disruption of the protective barrier and are accompanied by a number of reactions that change the composition and properties of both the metal surface and the local environment. For example corrosion leads in the formation of oxides, diffusion of metal cations into the coating matrix, local pH changes, and existence of electrochemical potential [23].

The study of corrosion of mild steel and iron is a matter of tremendous theoretical and practical concern and as such has received a considerable amount of interest. To this end, the use of corrosion inhibitors in order to restrain the corrosion attack on metallic materials has attracted the interest of the scientific community. Inhibitors are often added in industrial processes to secure metal dissolution from acid solutions (acid cleaning, acid descaling, acid pickling). Standard anticorrosion coatings (inorganic or organic) developed till date, passively prevent the interaction of corrosion species and the metal. The use of inhibitors is one of the best options to protect metals against corrosion [1], [23].

Corrosion protection highly depends on the interaction between the inhibitor and the metal surface. Corrosion inhibitors can be divided in two broad categories: a) namely, those that enhance the formation of a protective oxide film through an oxidizing effect that change the activation barriers of the anodic and cathodic reaction of the corrosion process and b) those that inhibit corrosion by selectively adsorbing on the metal surface and creating a barrier that prevents access of corrosive agents to the metal surface.

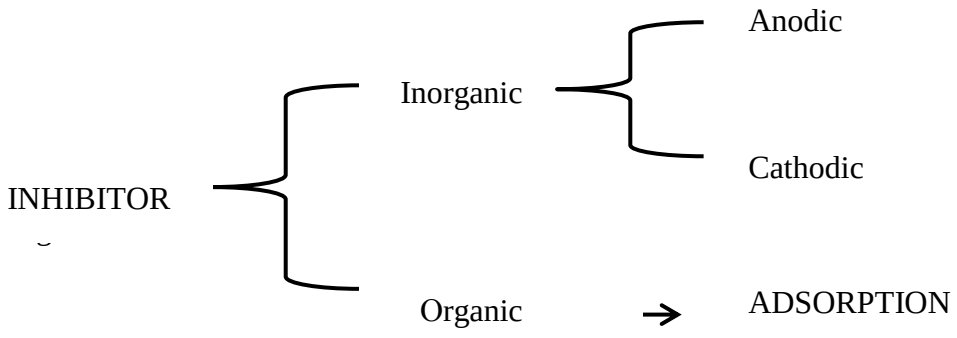

The inorganic corrosion inhibitors for example the anodic inhibitors act by reducing anodic reaction, blocking the anode reaction and supporting the natural reaction of metal surface's passivation, due to a formation of a film absorbed on the metal. The inhibitors react with the corrosion product that has initially formed, resulting in a cohesive and insoluble film on the surface. The cathodic inhibitors prevent the occurrence of the cathodic reaction of the metal. On the other hand the organic inhibitors act as cathodic, anodic or together, as cathodic and anodic. Nevertheless, as a general rule, they act through a process of surface adsorption. Naturally, the occurrence of molecules exhibiting a strong affinity for metal surfaces compounds showing good inhibition efficiency and low environmental risk. These inhibitors build up a protective hydrophobic film adsorbed on the metal surface, which provides a barrier to the dissolution of the metal in the electrolyte [2].

1.3 ADSORPION INHIBITORS

Organic and inorganic compounds might be used as adsorption inhibitors. Despite the promising findings about possible corrosion inhibitors, most of these are not only expensive but also toxic and non-biodegradable thus causing pollution problems and environmental hazards. Historically, the development of corrosion inhibitors has always been determined by their effectiveness, and they were often based on ecologically problematic heavy metal. Inorganic compounds such as chromate, dichromate, nitrite and nitrate are widely used as corrosion inhibitors in several media for different metals and alloys; on the other hand, the biotoxicity of these products, especially chromate, is well documented as well as their non-environmental-friendly characteristics which limit their application [7]. Hence, these deficiencies have prompted a continuing search for their replacement and researchers are focusing on non-toxic organic compounds. Possibilities include plant extracts, some drugs and other natural occurring products [8].

The initial mechanism in any inhibition process is the adsorption of the inhibitor on the metal surface. The adsorption process depends on the electronic characteristic and the geometry of the adsorbate molecules, the chemical composition of the solution, nature of the metal surface, type of environment, temperature of the reaction and on the electrochemical potential at the metal solution interface. A careful study of the adsorption

process of an inhibitor on the metal surface needs to take into consideration all the necessary factors. In the selection of potential corrosion inhibitors, the most interesting factors to take into consideration include the geometric properties and electronic properties of the compound. The geometry of the molecule has strong influence on the metal surface as it informs for the optimal way by which the inhibitor might cover the metal surface. Compounds that have planar geometry often have higher inhibition efficiency than corresponding compounds with less planar geometry. Researchers have shown that the length of alkyl chain had influence on molecular reactivity and the presence of indole ring advanced the reactivity [3].

The adsorption requires the existence of attractive forces between the adsorbate inhibitor and the metal. According to the type of forces, adsorption can be physisorption or chemisorption depending on the adsorption strength. Physisorption process is due to electrostatic attractive forces between inhibiting ions or dipoles and the electrically charged surface of the metal, absence of chemical bonds the molecule retains its gas phase. Chemisorption is a process which involves interaction between unshared electron pairs or π electrons with the metal, in order to form a coordinate type of bond. When chemisorption takes place, one of the reacting species acts as an electron pair donor and the other one acts as an electron pair acceptor [4].

The structure of the inhibitor's coating depends on the metallic surface's geometry while the tendency of the molecule to react with the substrate is related to the electronic properties of the surface. In particular, these electronic interactions depend strongly on the electron density distribution in the inhibitor and the metal surface. Regions on the molecule that have high electron density would preferably donate electrons to the partially filled or the vacant d orbitals of the metal, resulting in a donor-acceptor bond [3]. The inhibitor's adsorption occurs with the existence of active centers such as: a) P, S, N and O atoms, b) double or triple bonds and c) aromatic rings [4]. Molecules that have functional groups with high electron density have greater tendency to adsorb onto the metal surface, and include molecule with heteroatom functional groups (i.e. –C-O, -N=N and –NR2) conjugated π and aromatic π systems [4]. The number of lone pairs of electron and loosely bound π- electrons in those functional groups are the key structured features that determine the inhibition efficiency. Availability of non-bonded (lone pair) and p-electrons in inhibitor molecules facilitate electron transfer from the inhibitor to the metal. A coordinate covalent bond

depends upon the electron density on the donor atom of the functional group and also the polarizability of the group. In previous researches, most attention was paid to the mechanism of adsorption and also to the relationship between the structure of inhibitors, their adsorption on the metal surface and their inhibition efficiencies on the macroscopic level. Detailed study of organic corrosion inhibitors, has found that the inhibition efficiencies depend on some physicochemical properties, such as functional groups, steric effects, electronic density of the donor atom, π orbital character and corrosive environment. Therefore, theoretical prediction of the efficiency of corrosion inhibitors has become very popular [5]. The general trend in the inhibition efficiency of molecules containing heteroatoms is such that O<N<S<P. This trend is probably related to the tendency of an atom to donate electrons and is therefore related to the electronegativity of the atom. Oxygen has the highest electronegativity and therefore the least tendency to donate electrons while Phosphorus has the least electronegativity and the highest tendency to donate electrons [3].

Summarizing, excellent inhibitors are constituted by those who can donate electrons to unoccupied d orbitals of metal surface to form coordinate covalent bonds and can also accept free electrons from the metal surface by using their antibonding orbitals to form feedback bond. The inhibitory activity of these molecules is accompanied by their adsorption. Free electron pairs on heteroatoms or π electrons are readily available for sharing to form a bond and act as nucleophile (donate e^-) centers of inhibitor molecules and greatly facilitate the adsorption process over the metal surface whose atoms act as electrophiles (accept e^-) [6].

1.3.1 Organic Inhibitors

Organic compounds contain heteroatoms such as nitrogen, sulphur and oxygen along with multiple bonds in the molecules have been reported to inhibit corrosion of metals. The inhibiting action of these organic compounds is usually attributed to their interactions with the metal surface via their adsorption. Polar functional groups are regarded as the reaction center that stabilizes the adsorption process [9]. The power of the inhibition depends on the molecular structure of the inhibitor. Organic compounds which

can donate electrons to unoccupied d orbital of metal surface to form coordinate covalent bonds and can also accept free electrons from the metal surface by using their anti-binding orbital to form feedback bonds constitute excellent inhibitors [6].

Organic inhibitors offer protection by adsorbing and forming a protective film on the metal surface. Usually, there is a polar group in the organic molecule that adsorbs on the metal and a non-polar hydrophobic chain oriented perpendicular to this surface. These chains act, on the one hand, by repelling aggressive contaminants dissolved in the pore solution and, on the other, by forming a barrier on the metallic surface.

Among the organic inhibitors, natural plant extracts are used (from Aloe Vera to radish leaves). Most of them contain hetero-atoms such as N, S, P and O and can thus form protective films. Among green inhibitors, studies on lanthanide salts, natural polymers, such as guar gum and starch, and bio-mimicking green inhibitors, such as amino acids, were conducted [10].

1.3.2 Amino acids as inhibitors

Amino acids are attractive as inhibitors because they are biodegradable, non-toxic, relatively cheap, easy to produce with purities greater than 99% and environmentally friendly [11], [12]. They are components of living organics and are precursors for protein formation. Several researchers have investigated the inhibitory potential of some amino acids and the results obtained have given some hope for the use of amino acids as green corrosion inhibitors [8].

Amino acids are organic compounds containing nitrogen atoms with free electron pairs that are potentional sites for bonding with copper and iron surfaces and enable inhibiting action. Also, there is a possibility of introduction of other heteroatoms and groups in molecules of these compounds, so there is a wide range of derivatives that exhibit good inhibition characteristics.

Certain amino acids have already been tested as corrosion inhibitors not only experimentally but also using semiempirical or DFT methods [6], [13]-[16]. However, to our knowledge, no DFT study concerning L-glutamine as corrosion inhibitor of Cu (111) surfaces has been ever reported in the literature.

1.4 AMINO ACIDS

Amino acids are biologically important organic compounds composed of amine (-NH_2) and carboxylic (-COOH) functional groups, along with a side-chain specific to each amino acid. The key elements of an amino acid are carbon, hydrogen, oxygen and nitrogen, though other elements are found in the side-chains of certain amino acids. About 500 amino acids are known and can be classified in many ways (structural functional groups locations, polarity, pH level etc). Outside proteins, amino acids perform critical roles in processes such as neurotransmitter transport and biosynthesis. Because of their biological significance, amino acids are important in nutrition and are commonly used in nutritional supplements, fertilizers and food technology. Industrial uses include the production of drugs, biodegradable plastics and chiral catalysts [18],[19].

1.5 L-GLUTAMINE

Glutamine is one of the 20 amino acids encoded by the standard genetic code. It is an amino acid just like protein. L-glutamine is a conditionally essential amino acid present abundantly throughout the body and is involved in many metabolic processes. It is synthesized from glutamic acid and ammonia. It is the principal carrier of Nitrogen in the body and is an important energy source for many cells [32].

Glutamine is produced in the muscles and is distributed by the blood to the organs that need it. It might help digestive function, the immune system and other essential processes in the body, especially in times of stress. It is also important for providing nitrogen and carbon to many different cells in the body and removing excess ammonia (a common waste product in the body). It also helps your immune system function and may be needed for normal brain function and digestion [19].

L-Glutamine is very stable as a dry powder and as a frozen solution. In liquid media or stock solutions, however, L-glutamine degrades relatively rapidly [34]. L-glutamine contains the backbone CO_2CHNH_2 and an uncharged side chain $CH_2CH_2CONH_2$. The backbone consists of charged groups, while the sidechain amide group is a dipole system.

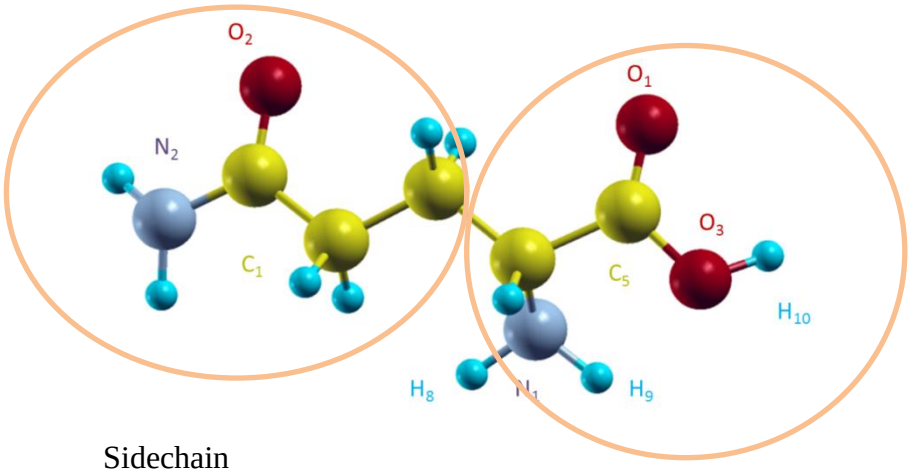

Figure 1.1 : Structure of L-glutamine

1.6 Aim of this work

Taking into account the importance of the Cu surfaces' protection from corrosion and the ability of L-glutamine to act as organic corrosion inhibitor, the adsorption of this molecule on the metallic surface becomes critical.

In this present study, we are investigating the adsorption of amino acid L-glutamine on the energetically favored Cu (111) surface through Density Functional Theory calculations. We are exploring the structural and electronic properties of the free and the deposited molecules on the metallic surface focusing in the investigation of the planar or vertical alignment along with the chemical bonding preferences. The results of this thesis may enlighten the mechanisms related to the protection of metallic surfaces from corrosion.

2. COMPUTATIONAL DETAILS

2.1 THE SCHRÖDINGER EQUATION

The Schrodinger equation is a linear 2nd grade ordinary differential equation and its solution is a wavefunction Ψ(r, t) that describes successfully the state of a system. The Schrodinger equation depends on both time and space. Usually the most problems don't depend on time so we can use the time independent form of Schrodinger equation:

$$\hat{H}\Psi=E\Psi, \tag{2.1}$$

where H is the Hamiltonian operator consisting of the two following terms which describe the kinetic and the dynamic potential energy:

$$H = -\frac{\hbar^2}{2m}\vec{\nabla}^2 + V(\vec{r}) \quad , \tag{2.2}$$

Ψ is the wavefunction defined over space and E is related to the total energy of the system.

The Schrodinger equation is an equation of eigenvalues. Each eigenvalue represent a different energy state of the system and the state where the total energy is minimized it is called ground state.

2.2 THE MANY BODY PROBLEM

In a real system the Schrodinger equation should be solve for all the atoms' nuclei and electrons that is referred as the many body problem. In these cases, the Hamiltonian operator should describe the kinetic energy of the electron and the nuclei while the

dynamic potential must cover all pair interactions. So the Hamiltonian operator for a system consisting of nuclei and electrons will have the form:

$$H=T_N(R)+T_e(r)+V_{eN}(r,R)+V_{NN}(R)+V_{ee}(r) \quad (2.3)$$

Where:

$$T_N(R) = -\hbar^2 \sum_I \frac{\nabla_I^2}{2M_I} \quad (2.4)$$ Nuclei kinetic energy

$$T_e(r) = -\frac{\hbar^2}{2m} \sum_i \nabla_i^2 \quad (2.5)$$ Electrons kinetic energy

$$V_{ee}(r) = \frac{1}{2} \sum_{i \neq j} \frac{e^2}{R_{ij}} \quad (2.6)$$ Electron- electron Coulomb interactions

$$V_{NN}(R) = \frac{1}{2} \sum_{I \neq J} \frac{Z_I Z_J e^2}{R_{IJ}} \quad (2.7)$$ Nucleus- nucleus Coulomb interaction

$$V_{eN}(r,R) = -\frac{1}{2} \sum_{Ii} \frac{Z_I e^2}{R_{Ii}} \quad (2.8)$$ Coulomb interaction between the nuclei and the electrons

The Schrodinger equation Ψ of the N particles depend on the coordinates of the electrons r_i and the nuclei R_i:

$$\Psi = \Psi(r_i, R_I) = (r_1, r_2, ..., r_k, R_1, R_2, ..., R_M) \quad (2.9)$$

The Hamiltonian operator is now complicated enough to find a solution. For that reason we have to make some approximations.

2.2.1 The Born-Oppenheimer approximation

The first approximation that used for the solution of this complicated Hamiltonian operator, is the Born-Oppenheimer approximation. Because of the large masses of the nuclei, they move much slower than the electrons so it can be considered that nuclei are fixed during the electrons' motion in the field of the nuclei. So the nuclei kinetic energy is zero and their potential energy is a constant. The Hamiltonian operator for the electrons and the Schrodinger equation become:

$$\hat{H}_e \psi(r, R_I) = [T_e(r) + V_{eN}(r,R) + V_{ee}(r)] \psi(r,R_I) = E_e(R) \psi(r,R_I) \qquad (2.10)$$

Where the Hamiltonian operator H consists of: the kinetic energy of electrons $T_e(r)$, the nuclei-electron Coulomb interaction $V_{eN}(r, R)$ and the electron- electron Coulomb interaction V_{ee}. For nuclei the vibration and rotation movement is only considered.

2.2.2 One electron approximation

The one-electron approximation refers to the solution of the one-electron Schrodinger equation, separately for each electron, considering a common mean field potential U(r) that describes every interaction between the particles and every external potential that might act in the system. The single-particle Schrodinger equations take the form:

$$-\frac{\hbar^2}{2m}\nabla^2\phi_i(r) + U(r)\phi_i(r) = \varepsilon\phi_i(r) \qquad (2.11)$$

2.2.3 Hartree approximation

In the Hartree Approximation the electron-electron interaction is described using the electron eigenstates $\varphi_i(r)$ while the total Hamiltonian wavefunction Ψ^H can be written as a product of these single particle states.

$$\Psi^H = \phi_1(r_1)\phi_2(r_2)...\phi_N(r_N) \qquad (2.12)$$

The mean field potential U(r) consists of the following parts:

a) the nuclei-electron Coulomb interaction:

$$U_{ion}(r) = -\sum_a \frac{Z_a e^2}{4\pi\varepsilon_o |r - d_a|} \qquad (2.13)$$

Where r is the coordinate of electron and the charge on the nucleus at d_a, is Z_a

b) the electron-electron Hartree interaction:

This second part of the electrons contribution is due to the electron- electron interactions and it is a Coulomb interaction that can be described using the charge density ρ(r). This potential is known as Hartree potential and it changes for every electron:

$$U_i^H(r) = e^2 \int dr' \left[\rho(r') - \rho_i(r')\right] \frac{1}{|r - r'|} \qquad (2.14)$$

The electrons have been considered as independent particles so their density charge ρ(r) can be calculated by their one electron eigenstates:

$$\rho(r) = \sum_i |\phi_i(r)|^2 \qquad (2.15)$$

So the potential of the single-particle is the sum of the electron-nuclei interaction and the electron-electron interaction:

$$U_i(r) = U_{ion}(r) + e^2 \underbrace{\sum_{j \neq i} \int dr' \left|\phi_j(r')\right|^2 \frac{1}{\left|r - r'\right|}}_{U_H} \qquad (2.16)$$

The average total energy for a state specified by a particular Ψ, is the expectation value of H, that is:

$$E^H = \left\langle \Psi^H \middle| H \middle| \Psi^H \right\rangle = \sum_i \int dr \phi_i^*(r) \left(-\frac{\hbar^2}{2m_e} \nabla_r^2 + U_{ion}(r) \right) \phi_i(r) + \frac{e^2}{2} \sum_i \sum_{j(\neq i)} \int dr dr' \frac{\left|\phi_i(r)\right|^2 \left|\phi_j(r')\right|^2}{\left|r - r'\right|} \qquad (2.17)$$

2.2.4 Hartree-Fock approximation

The ground state may be found by searching all possible wavefunctions that minimizes the total energy. In the Hartree-Fock theory the Ψ^{HF} is assumed an antisymmetric product of functions (φ_i) which depend on the single electron coordinates:

$$\Psi^{HF}(\{r_i\}) = \frac{1}{\sqrt{N!}} \begin{vmatrix} \phi_1(r_1) & \phi_1(r_2) & \cdots & \phi_1(r_N) \\ \phi_2(r_1) & \phi_2(r_2) & \cdots & \phi_2(r_N) \\ \vdots & \vdots & \ddots & \vdots \\ \phi_N(r_1) & \phi_N(r_2) & \cdots & \phi_N(r_N) \end{vmatrix} \qquad (2.18)$$

The ground state orbitals are determined finding the minimum of the energy. This leads to the Hartree- Fock (or SCF) equations:

$$\varepsilon_i \phi_i(r) = \left(-\frac{1}{2}\nabla^2 + U_{ion}(r) \right) \phi_i(r) + e^2 \sum_{j \neq i} \int dr' \frac{\left|\phi_j(r')\right|^2}{\left|r - r'\right|} \phi_i(r) - e^2 \sum_{j \neq i} \delta_{s_i s_j} \int dr' \frac{\phi_j^*(r')\phi_i(r')}{\left|r - r'\right|} \phi_j(r)$$

(2.19)

The first term is the sum of electrons' kinetic energy and the nuclei-electron Coulomb interaction, the second term is the Hartree potential while the third term is the non-local exchange potential.

2.3 DENSITY FUNCTIONAL THEORY

Density functional theory (DFT) is a computational quantum mechanical method used in physics, chemistry and materials science for the investigation of the electronic structure (principally the ground state) of many-body systems. Using this theory, the properties of a many-electron system can be determined by a functional, which describes the system's electron density. DFT is among the most popular and versatile methods available in condensed-matter physics, computational physics and computational chemistry.

2.3.1 The electron density

In the simple case where the spins' coordinate is omitted the system's electron density is described by the form:

$$\rho(r) = N \int \left| \Psi_o\left(r, r_2, ..., r_N\right) \right|^2 dr_2 ... dr_N \qquad (2.\ 20)$$

Here in Ψ_0 is the many-particles wavefunction of the ground state.

2.3.2 Hohenburg-Kohn theorems

In 1964 Hohenburg and Kohn proved the two basic theorems. The first theorem states that *the electron density ρ (r) determines the external potential*. So it is easily proven that since the external potential fixes the Hamiltonian operator, the full many particle ground state is a unique functional of ρ(r). This leads to the conclusion that ρ(r) determines N and the external potential hence all the properties of the ground state, i.e. the kinetic energy and the total energy. So the total energy will be:

$$E_0=E[\rho_0(r)], \tag{2.21}$$

In addition, we can assume the functional $F_{HK}[\rho]$ which contains the functional of kinetic energy K[ρ] and the functional for the electron-electron interaction V_{ee} [ρ].

The second theorem establishes a variational principle; *for any positive definite trial density* ρ_t *such that* $\int \rho(r)dr = N$, *then* $E_0 \leq E[\rho_t]$. This theorem restricts density functional theory to studies of the ground state.

2.3.3 The Kohn-Sham equations

The total energy in the Schrödinger equation contains the following terms: the kinetic energy T[ρ(r)], the interaction with the external potential $U_{ion}(r)$, ~~and~~ the electron-electron V_{ee} (ρ(r)) and the exchange-correlation interaction $E_{xc}(\rho(r))$ which are defined through the system's charge density ρ(r). So the energy functional is:

$$E(\rho(r))= T(\rho(r))+U_{ion}(\rho(r))+ V_{ee}(\rho(r))+ E_{xc}(\rho(r)) . \tag{2. 22}$$

Kohn and Sham introduced a fictitious system of N non-interacting electrons to be described by a single determinant wavefunction using the N *φi* orbitals. In this system the kinetic energy and electron density are exactly expressed through the *φi*:

$$T_s[\rho(r)] = -\frac{1}{2}\sum_{i=1}^{N}\int \phi_i^*\nabla^2\phi_i \, dr \tag{2. 23}$$

The electron density can be calculated using the expression: $\rho(r) = \sum_{i=1}^{N} |\phi_i(r)|^2$. (2.24)

The electron-electron interaction will be the classical Coulomb interaction – or Hartree energy:

$$U^H = \frac{1}{2}\int\int \frac{\rho(r)\rho(r')}{|r-r'|} dr dr' \qquad (2.25)$$

Finally the functional of energy will have the form:

$$E[\rho(r)] = T_s[\rho(r)] + \frac{1}{2}\int\int \frac{\rho(r)\rho(r')}{|r-r'|} dr dr' + E_{XC}[\rho(r)] + \int \rho(r) U_{ext}(r) dr \qquad (2.26)$$

2.3.4 The local density approximation (LDA)

The local density approximation (LDA) is the basis of all exchange-correlation functionals. The central idea of LDA is the assumption that we can write EXC in the following form:

$$E_{XC}[\rho(r)] \approx \int \varepsilon_{XC}(\rho(r))\rho(r) dr \qquad (2.27)$$

Here, ε_{XC} (ρ(r)) is the exchange-correlation energy per particle of a uniform electron gas of density ρ(r). This energy per particle is weighted with the probability ρ(r) that there is an electron at this position [39], [40].

3. SOFTWARE

3.1 SIESTA PROGRAM

The calculations performed with the Spanish Initiative for Electronic Simulations with Thousands of Atoms (SIESTA), in the generalized gradient approximation (GGA) for exchange and correlation.

SIESTA is both a method and its computer program implementation, to perform efficient electronic structure calculations and ab initio molecular dynamics simulations for molecules and solids. A very important feature of the code is that its accuracy and cost can be tuned in a wide range, from quick exploratory calculations to highly accurate simulations matching the quality of other approaches, such as plane-wave and all-electron methods. The possibility of treating large systems with some first-principles electronic-structure methods has opened up new opportunities in many disciplines. The SIESTA program is distributed freely to academics and has become quite popular, being increasingly used by researchers in geosciences, biology, and engineering (apart from those in its natural habitat of materials physics and chemistry).

It uses the standard Kohn-Sham self-consistent density functional method in the local density (LDA) or generalized gradient (GGA) approximations. It employs norm-conserving pseudopotentials in their full nonlocal form and atomic orbitals as basis set allowing unlimited multiple-zeta and angular momenta, polarization and off-site orbitals. It projects the electron wavefunctions and density onto a real-space grid in order to calculate the Hartree and exchange-correlation potential and their matrix elements.

SIESTA code provides total and partial energies, atomic forces, stress tensor, electric dipole moment, atomic, orbital and bond populations, electron density, geometry relaxation, local and orbital-projected density of states, dielectric polarization,spin polarized calculations, constant-temperature molecular dynamics (Nose thermostat).

The directory contains basically .fdf files and the appropriate pseudopotential generation input files (.psf) that can be found through the SIESTA webpage [41].

3.1.1 The flexible data format (FDF)

The main input file contains all the physical data of the system and the parameters of the simulation to be performed. This file is written in a special format called FDF. This format allows data to be given in any order, or to be omitted in favor of default values. One .fdf file that used in our calculations is presented in Figure [1].

```
# FDF for Cu surface111  a =3.615Ang

SystemName          cu111_glut_110p_ontop       # Descriptive name of the system
SystemLabel         cu111_glut_110p_ontop        # Short name for naming files

WriteSiestaDim        false       # If true: writes dimensions and stops

WriteMullikenPop      1           # to write population analysis

NumberOfSpecies       5           # Number of species

NumberOfAtoms         170        # Number of atoms

PAO.BasisType         split       # Type of PAO basis set
PAO.EnergyShift       50 meV
PAO.BasisSize         DZP         # (DZP) Double-z + polarization

%block  Chemical_Species_label
       1  6   C
       2  1   H
       3  8   O
       4  7   N
       5 29   Cu
%endblock Chemical_Species_label

%block PAO.basis        # Define Basis set
C     3       .35201
n=2   0   2   E    50.37145     5.22551
     5.43077     3.08484
     1.00000     1.00000
n=2   1   2   E    13.53326     6.81234
     6.83094     3.01366
     1.00000     1.00000
n=2   2   1   E   110.78225      .01065
     5.04748
     1.00000
H   1
     0   2    P
     0.000000000   0.000000000
     0.000000000   0.00000000
O   2
     0   2
     0.0000000    0.0000000
     0.0000000    0.0000000
     1   2    P
     0.00000000   0.0000000
     0.00000000   0.0000000
N   2
     0   2
     0.0000000    0.0000000
     0.0000000    0.0000000
```

```
LatticeConstant       1.00 Ang

%block LatticeVectors
     13.2825      0.0000      0.0000
      0.0000     12.7810      0.0000
      0.0000      0.0000     50.0000
%endblock LatticeVectors

%block kgrid_Monkhorst_Pack
 2   0   0       0.000
 0   2   0       0.000
 0   0   1       0.000
%endblock kgrid_Monkhorst_Pack


#SpinPolarized         true

MeshCutoff            100. Ry        # Mesh cutoff. real space mesh (Ry)

# SCF options
MaxSCFIterations      100            # Maximum number of SCF iter

DM.MixingWeight       0.01         # New DM amount for next SCF cycle
DM.Tolerance          1.d-2         # Tolerance in maximum difference
#DM.Tolerance          1.d-4         # Tolerance in maximum difference
                                    # between input and output DM
DM.NumberPulay        3
DM.UseSaveDM          true          # to use continuation files

NeglNonOverlapInt     false         # Neglect non-overlap interactions

SolutionMethod        diagon        # OrderN or Diagon
ElectronicTemperature 300 K         # Temp. for Fermi smearing (Ry)


MD.TypeOfRun          cg            # Type of dynamics:
MD.UseSaveXV          true          #  try to use Que.DZP.XV
MD.UseSaveCG          true          #  try to use Que.DZP.XV

MD.NumCGsteps         200           # Number of CG steps for
                                    #   coordinate optimization
MD.MaxCGDispl         0.2 Bohr      # Maximum atomic displacement
                                    #   in one CG step (Bohr)
#MD.MaxForceTol        0.15 eV/Ang  # Tolerance in the maximum
#MD.MaxForceTol        0.5 eV/Ang   # Tolerance in the maximum
 MD.MaxForceTol        0.05 eV/Ang  # Tolerance in the maximum
                                    #   atomic force (Ry/Bohr)


AtomicCoordinatesFormat  NotScaledCartesianAng   # Format for coordinates
```

```
AtomicCoordinatesFormat  NotScaledCartesianAng   # Format for coordinates

%block AtomicCoordinatesAndAtomicSpecies
    0.00000000    0.00000000    6.26140020   5  Cu         1
    0.00000000   10.22480000    6.26140020   5  Cu         2
    0.00000000    2.55620000    6.26140020   5  Cu         3
    0.00000000    5.11240010    6.26140020   5  Cu         4
    0.00000000    7.66860010    6.26140020   5  Cu         5
   11.06870000   11.50290000    6.26140020   5  Cu         6
   11.06870000    1.27810000    6.26140020   5  Cu         7
   11.06870000    3.83430000    6.26140020   5  Cu         8
   11.06870000    6.39050010    6.26140020   5  Cu         9
   11.06870000    8.94670010    6.26140020   5  Cu        10
    2.21370010   11.50290000    6.26140020   5  Cu        11
    2.21370010    1.27810000    6.26140020   5  Cu        12
    2.21370010    3.83430000    6.26140020   5  Cu        13
    2.21370010    6.39050010    6.26140020   5  Cu        14
    2.21370010    8.94670010    6.26140020   5  Cu        15
    4.42749980    0.00000000    6.26140020   5  Cu        16
    4.42749980   10.22480000    6.26140020   5  Cu        17
    4.42749980    2.55620000    6.26140020   5  Cu        18
```

Figure [3.1]: FDF file

Here follows a description of the variables that can be defined in Siesta Input file.

Firstly, a descriptive name and a nickname of the file are defined in the system name and the system label respectively.

In the fdf file, the number of species and the number of atoms are introduced. In ChemicalSpeciesLabel is specified the different chemical species that are present, assigning them a number for further identification by the SIESTA program.

```
%block Chemical_Species_label
1   6   C
2   1   H
3   8   O
4   7   N
5  29   Cu
%endblock Chemical_Species_label
```

The first number in a line is the species number, it is followed by the atomic number and then by the desired label. This label will be used to identify corresponding files, namely, pseudopotential file, user basis file.

In WriteMullikenPop is determined the Mulliken population analysis printed:

- 0 = None
- 1 = atomic and orbital charges
- 2 = 1 + atomic overlap pop.
- 3 = 2 + orbital overlap pop.

In our case, it is determined by the integer 1.

In addition the type of PAO basis set is defined in the fdf file. In this study, split valence scheme for double zeta basis plus polarization orbitals has been used. Also, the PAO.EnergyShift is in 50 meV. Hereupon, the different value of PAO.basis for each species is defined (Figure [2]).

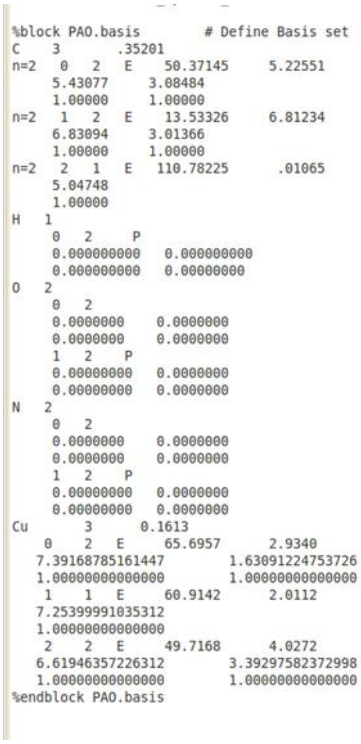

```
%block PAO.basis        # Define Basis set
C    3       .35201
n=2   0   2   E    50.37145     5.22551
     5.43077     3.08484
     1.00000     1.00000
n=2   1   2   E    13.53326     6.81234
     6.83094     3.01366
     1.00000     1.00000
n=2   2   1   E   110.78225      .01065
     5.04748
     1.00000
H   1
     0   2     P
     0.000000000   0.000000000
     0.000000000   0.00000000
O   2
     0   2
     0.0000000    0.0000000
     0.0000000    0.0000000
     1   2    P
     0.00000000   0.0000000
     0.00000000   0.0000000
N   2
     0   2
     0.0000000    0.0000000
     0.0000000    0.0000000
     1   2    P
     0.00000000   0.0000000
     0.00000000   0.0000000
Cu       3      0.1613
    0    2   E     65.6957      2.9340
   7.39168785161447        1.63091224753726
   1.00000000000000        1.00000000000000
    1    1   E     60.9142      2.0112
   7.25399991035312
   1.00000000000000
    2    2   E     49.7168      4.0272
   6.61946357226312        3.39297582372998
   1.00000000000000        1.00000000000000
%endblock PAO.basis
```

Figure [3.2]: PAO basis for each species as defined in .fdf file

SIESTA uses a finite 3D grid for the calculation of some integrals and the representation of charge densities and potentials. Its fitness is determined by its plane-wave cutoff, as given by the MeshCutoff option. Herein, MeshCutoff is 70 Ry and 100 Ry depending on the system.

SpinPolarized is defined as true.

Consequently, the size of the cell itself is specified, using some combination of the options LatticeConstant and LaticeVectors. LatticeConstant (1 Ang) is to define the scale of the lattice vectors. The cell vectors are read in units of the lattice constant and they are read as a matrix CELL (ixyz, ivector), each vector being one line. The cell vectors as defined in our calculations are shown in Figure [3].

In addition, in our calculations the kgrid_Monkhorst_Pack option was used for the k-point grid. Specified as an integer matrix and a real vector, Figure [3] shows the matrix that was used:

Temperature for Fermi-Dirac was set at 300 K.

The maximum number of self-consistent field iterations per time step was defined as 100.

```
LatticeConstant       1.00 Ang

%block LatticeVectors
     13.2825      0.0000      0.0000
      0.0000     12.7810      0.0000
      0.0000      0.0000     50.0000
%endblock LatticeVectors

%block kgrid_Monkhorst_Pack
 2   0   0       0.000
 0   2   0       0.000
 0   0   1       0.000
%endblock kgrid_Monkhorst_Pack
```

Figure [3.3]: Lattice vectors and kgrid_Monkhorst_Pack as defined in .fdf file

In the fdf file the DM.Tolerance is the tolerance of the density matrix. When the maximum difference between the output and the input on each element of the DM in a SCF cycle is smaller than DM.Tolerance, the self-consistency has been achieved. DM.MixingWeight is the amount of output Density Matrix to be used for the input Density Matrix of next SCF cycle.

Several options for MD and structural optimizations are implemented, selected by MD.TypeOfRun. In our calculations, CG (coordinate optimization by conjugated gradients) was selected.

MD.NumCGsteps is referred to the maximum number of conjugate gradient minimization moves. The minimization will stop if tolerance is reached before. The number of CG steps was set as 200. The maximum atomic displacement in one CG step was set as 0.2 Bohr.

The force tolerance in coordinate optimization is defined in MD.MaxForceTol. Run stops if the maximum atomic force is smaller than this amount. The atomic force that used in our study is 0.04 eV/Ang.

Finally, the atomic coordinates of the system's atoms were inserted in the fdf file. The unit of measurement of the coordinates is Angstrom.

3.1.2 Standard Output

Siesta writes a log of its workings to standard output, which is usually redirected to an “output file”. The program starts writing the version of the code which is used. Then, the input FDF file is dumped into the output file. After that, the program reads the pseudopotentials and generates (or reads) the atomic basis set to be used in the simulation. These stages are documented in the output file.

The simulation begins and the output shows information of the MD (or CG) steps and the SCF cycles within. The user has the option to customize the input file, however, by defining different options that control the printing of information like coordinates, forces, k-points, etc.

Siesta uses pseudopotentials to represent the electron-ion interaction (as do most plane-wave codes and in contrast to so-called “all-electron" programs). The pseudopotentials will be read by Siesta from different files, one for each defined species.

In the CG operation, the program moves the atoms (and optionally the cell vectors) trying to minimize the forces (and stresses) on them. After a successful run of the program, you should have several files in your directory including the following: fdf.log, .ion, .XV, .STRUCT_OUT, .DM, .ANI, .EIG, .FA, .xml.

Siesta always produces a .STRUCT_OUT file with cell vectors in Å and atomic positions in fractional coordinates. The coordinates are always written in the SystemLabel.XV file, and overridden at every step. If WriteMDXMol defined as true, it causes the writing of an extra file named SystemLabel.ANI containing all the atomic coordinates of the simulation in a format directly readable by XMol and XCrysden for animation. Coordinates come out in Angstrom.

The Hamiltonian eigenvalues for the sampling k points are written in the SystemLabel.EIG file, which can be used for obtaining the Fermi level and the density states. The Hamiltonian eigenvectors corresponding to the k vectors, defined by the WaveFunckPoints descriptor, are dumped into the file SystemLabel.WFS, to be used by post processing utilities for handling the wavefunctions. In addition, the descriptor ProjectedDensityOfStates (block) instructs to write the total density of states (DOS) and

the projected density of states (PDOS) on the basis orbitals, between two given energies, in files SystemLabel.DOS and SystemLabel.PDOS respectively [41].

3.2 XCRYSDEN

As mentioned above, the file .ANI is readable by XCrysden. XC is a crystalline- and molecular-structure visualization program. The name of the program stands for Crystalline Structures and Densities and *X* because it runs under the X-Window environment. It facilitates a display of isosurfaces and contours, which can be superimposed on crystalline structures and interactively rotated and manipulated. It also possesses some tools for analysis of properties in reciprocal space such as interactive selection of k-paths in the Brillouin zone for the band-structure plots, and visualisation of Fermi surfaces. This program is free software.

In our study, the XCrysden was widely used for structure and charge density optimization.

3.3 XMAKEMOL

XMakemol is a mouse-based program for viewing and manipulating atomic and other chemical systems. It reads XYZ input and renders atoms, bonds and hydrogen bonds. Some of the features of XMakeMol are: animating multiple frame files, control over atom/bond sizes, exporting to XPM and Fig formats, editing the positions of subsets of atoms.

The XMakeMol was used in our study, for the purpose of rotating the molecules and having different desirable configurations. The new coordinates was given by the XMakeMol in a XYZ file.

3.4 XMGRACE

Grace is a 2D plotting tool for the X Window System and M*tif. Grace runs on practically any version of Unix-like OS, also known as Xmgr. Some of Xmgrace's features are: convenient point-and-click graphical user interface, precise control of graph features, support of cross-platform PNG, PNM, and JPEG formats, unlimited number of graphs, unlimited number of curves on a graph.

The graphs presented in this study are plotted through the Xmgrace.

3.5 SYSTEMS' COMPUTATIONAL DETAILS

We performed standard Kohn−Sham self-consistent density functional theory calculations within the SIESTA code using the following approaches: (i) local density approximation (LDA) with the exchange-correlation term taken from Ceperley−Alder data as parametrized by Perdew−Zunger and (ii) generalized gradient-corrected approximation (GGA) within the PBE (Perdew−Burke−Ernzerhof) for selective cases. Core electrons were replaced by norm-conserving pseudopotentials in the fully nonlocal Kleinman−Bylander form and the basis set was a linear combination of numerical atomic orbitals (NAOs) constructed from the eigenstates of the atomic pseudopotentials. An auxiliary real space grid equivalent to a plane-wave cutoff of 100 Ry was used. The self-consistency is achieved when the change in the total energy between cycles of the SCF procedure is below 10^{-4}eV, (energy convergence criterion), and the density matrix change criterion 10^{-4} is also satisfied.

The energetically favored Cu(111) was simulated using a five-layer (3x5) unit cell forming infinite slabs with {111} surface orientation, resulting 150 atoms as presented in Figure [1]. Periodic boundary conditions were applied while the system was sampled with four (2x2x1) in plane k-points and a vacuum of 20 Å. During the geometry optimizations, all atoms were relaxed, except the last two layers that were kept fixed, thus mimicking the bulk positions

The structure was considered as being fully relaxed when the magnitude of forces on the atoms was smaller than 0.04 eV/Å. The Cu (111) total energy was found to be : $\boldsymbol{E_{surface}}$ = -182737.4003 eV.

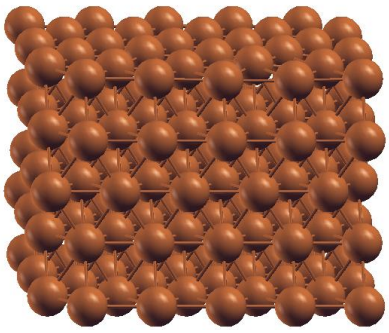

Figure [3.1]: Cu (111) surface

The L-glutamine was initially considered as an aligned molecule and using energy minimization its final configurations was optimized. Afterwards the molecule was softly deposited on the Cu (111) surface using several orientations as described in the following sessions.

Xcrysden was used for the optimization of the structures.

4. RESULTS AND DISCUSSION

4.1 L-GLUTAMINE

4.1.1 Structural properties

The amino acid L-glutamine was initially constructed with its chain aligned, Figure 1a and using energy minimization Density Functional Theory (DFT) calculations the equilibrium structure was received, Figure 1b. The L-glutamine's total energy was minimized until the forces between the atoms were less than 0.5 eV/ Å. Upon energy minimization the carbon chain of the molecule was curled while the H atoms formed their favored angles with the C and N atoms [28], [29]. Selective bond lengths between the atoms are shown in the Table [1].

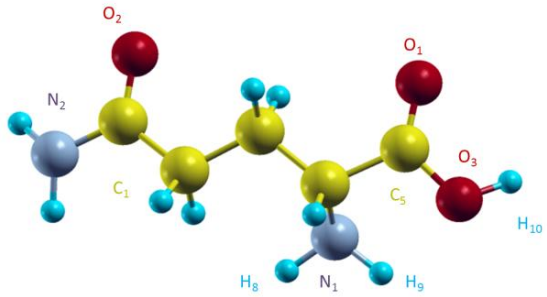

Equilibrium structure of L-glutamine

Figure [4. 1]: L-glutamine equilibrium configuration. Grey, yellow, red and blue balls stand for the N, C, O, and H atoms, respectively.

Table 4.1

Selective L-glutamine's bond lengths.

L-glutamine		Bond length (Å)
	Experimental (X-ray)[42]	equilibrium
N2-C1	1.338	2.5606
02-C1	1.243	2.3676
N1-C4	1.496	2.7599

01-C5	1.268	2.3275
03-C5	1.246	2.5132
C1-C2	1.515	2.8
C2-C3	1.524	2.8572
C3-C4	1.533	2.8588
C4-C5	1.543	2.876

Aiming to identify the molecular interactions and the molecule's active sites behavior, we studied the L-glutamine's electronic structure and we optimized these structures. Certain electronic structure parameters have been correlated with the effectiveness of adsorption-type inhibitors. These include the energy of the highest occupied molecular orbital (HOMO), the lowest unoccupied molecular orbital (LUMO) energy and the HOMO-LUMO energy gap [27].

The results of HOMO, LUMO Fermi level energy and total energy are shown in Table [2].

Table [4.2]

Values of E_{HOMO}, E_{LUMO}, Fermi level and total energy for L-glutamine's molecule.

Total energy (eV)	Fermi level (eV)	HOMO (eV)	LUMO (eV)	ΔE=LUMO-HOMO (eV)
-2779.7719	-3.8487	-5.74099	-1.71852	4.02247
Literature [6]		-5.68	-2.106	3.58

4.1.2 Electronic properties

The values of E_{HOMO} and E_{LUMO} are in a good agreement with other quantum chemical methods [6]. The HOMO energy characterizes the susceptibility of the molecule when it is attacked by electrophiles. High E_{HOMO} value indicates a tendency of the

molecule to donate electrons to appropriate acceptor molecules with low energy MO or empty electron orbital. Increasing values of E_{HOMO} are likely to indicate adsorption and therefore enhanced inhibition efficiency by an influence at the adsorbed layer through transport processes. The LUMO energy characterizes the propensity of the molecule towards attack by nucleophiles. Low value of E_{LUMO} indicates an electron accepting ability of an inhibitor molecule. The binding ability of an inhibitor to a metal surface increases with increasing E_{HOMO} and decreasing E_{LUMO} [6],[26],[27].

The geometry optimized structures and the optimized HOMO and LUMO of L-glutamine are presented in Figure [2]. Red and blue colours indicate particular isosurfaces at positive and negative values, respectively.

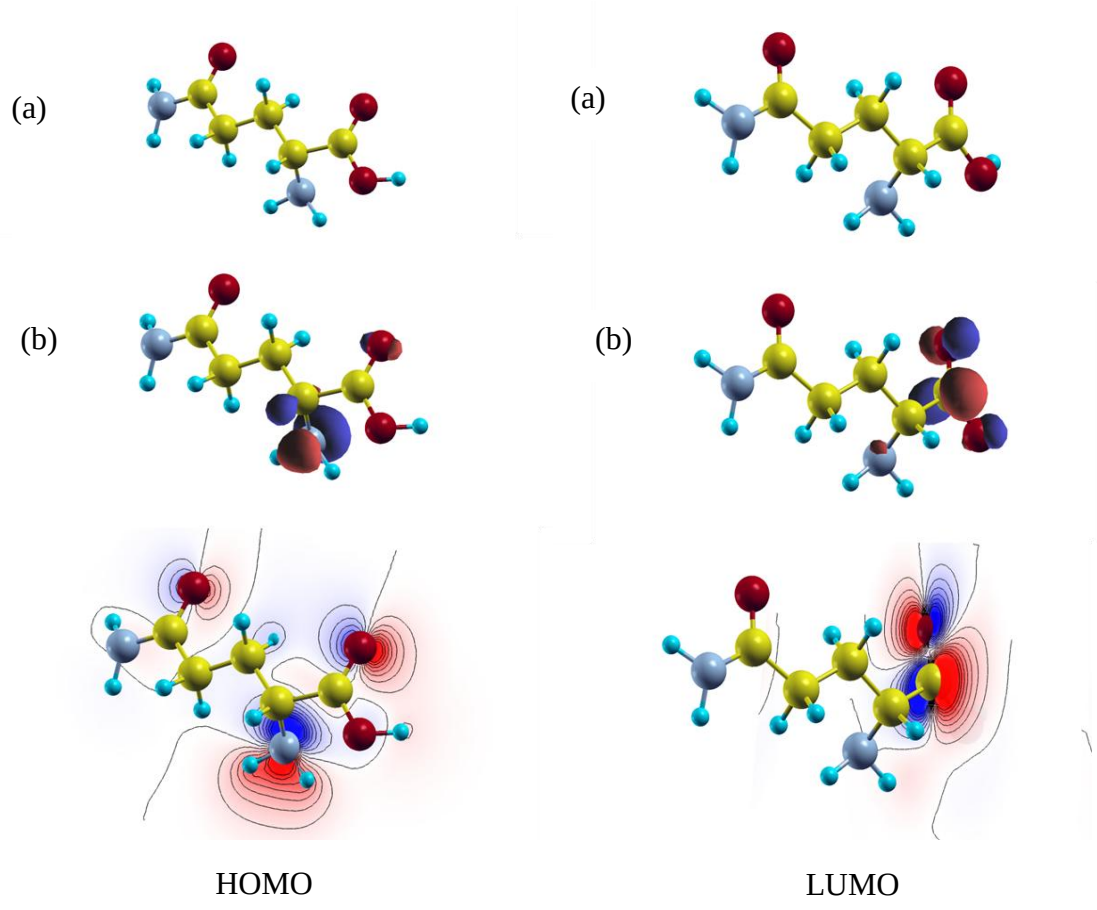

Figure [4.2]: Electronic properties of L-glutamine in HOMO and LUMO. The red (blue) color indicates isosurfaces of the wave function with positive (negative) sign. (a) optimized structure, (b) optimized electron density. Grey, yellow, red and blue balls stand for the N, C, O, and H atoms, respectively.

Figure [2] reveals that HOMO and LUMO of L-glutamine are saturated around the amide group of L-glutamine's backbone. The HOMO is found to exist mostly around backbone's

N and O atoms and less around C atoms and the LUMO is localized mostly around backbone's O and C atoms and less around N atom of L-glutamine. This is in agreement with the other studies of L-glutamine's electronic properties [6]. In addition, for both states the O and N p orbital are not hybridized and left as dangling bonds indicating that L-glutamine will probably interact with the metallic surface through them. In particular, hybridizations between the occupied *d* orbital of Cu (111) surface and the *p* orbital of L-glutamine are expected in line with the characteristic amino acids' adsorption chemical bonding on metallic surfaces [6].

4.2 L-GLUTAMINE ON CU (111) SURFACE

4.2.1 Structural properties

We performed DFT calculations in order to study the L-glutamine's adsorption mechanism. We firstly softly deposited the molecule on Cu (111) surface in several configurations in order to investigate the energetically favored configuration. The system's energy was minimized until the forces between the atoms were less than 0.5 eV/Å. Figure [3] represents the deposition of L-glutamine on Cu (111) surface.

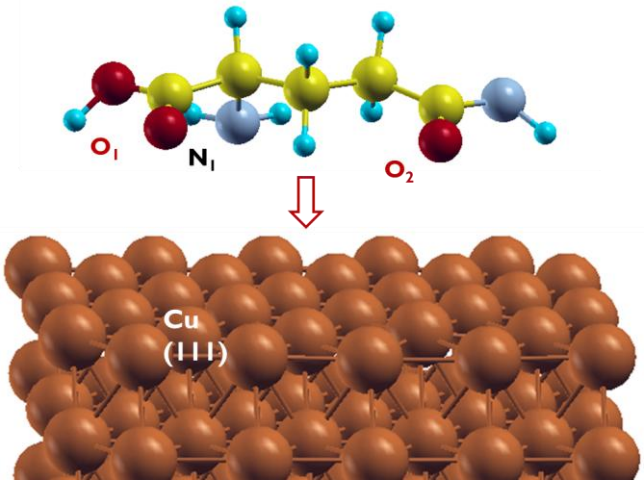

Figure [4. 3]: Representation of deposition of L-glutamine on Cu (111) surface. Grey, yellow, red, blue and orange balls stand for the N, C, O, H and Cu atoms, respectively.

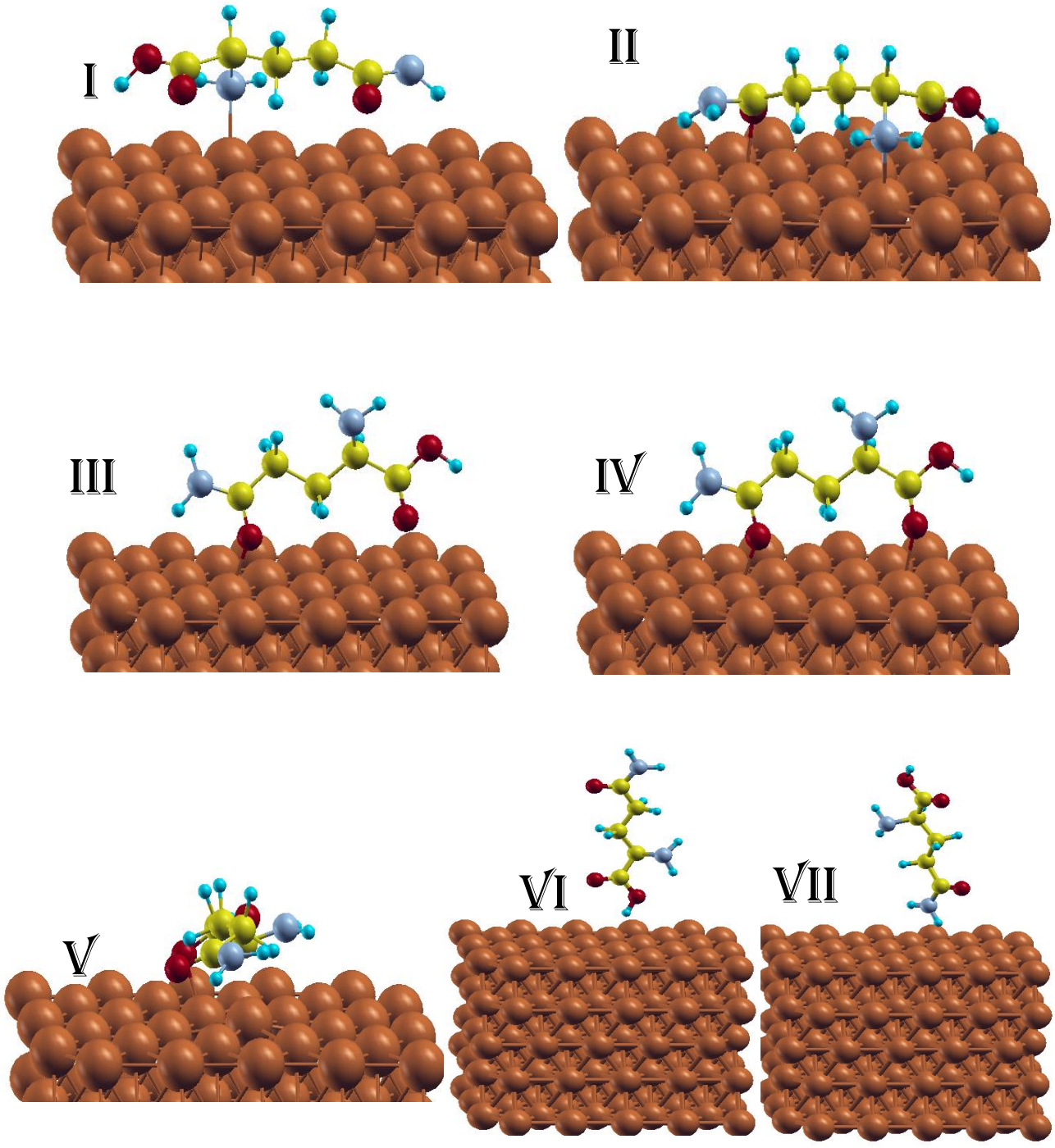

Figure [4.4] : Optimized configurations of L-glutamine on Cu (111) surface : (I), (II) parallel along the [110] site of Cu surface, (III),(IV) horizon and parallel the [110] site of Cu surface, (V) vertical the [110] site of Cu surface and (VI),(VII) vertical with O and N above the surface respectively. Grey, yellow, red, blue and orange balls stand for the N, C, O, H and Cu

The configurations of L-glutamine on Cu (111) surface are presented in Figure [4]. (I) and (II) shows the two on top sites along the [110] site of Cu surface having the N and O atoms "on top" of Cu atoms, (III) and (IV) the horizontal position of L-glutamine along the [110] site with the two O atoms toward the surface, (V) the vertical position along the [110] site and finally (VI) and (VII) show the vertical position of L-glutamine molecule on Cu (111) layer with the O atom and N atom above the surface respectively.

In order to appraise quantitatively the interaction between the molecule and the metallic surface, we calculated the binding energy between L-glutamine and Cu (111) surface using the following equation:

$$\boldsymbol{E_{binding} = E_{total} - \left(E_{surface} + E_{glut}\right)} \qquad \textbf{(4.1)}$$

herein, E_{total} is the total energy of the Cu surface together with the adsorbed inhibitor molecule, $E_{surface}$ is the total energy of the Cu surface and E_{glut} is the total energy of the L-glutamine molecule (Table 4). The values of the total and the binding energies are listed in Table 3. Configuration I is the most stable adsorption structure, showing the lowest energy, within the seven studied different configurations. The next favored configuration is II.

Table 4.3

Values of total energies and binding energies for the seven configurations

Configuration	I	II	III	IV	V	VI	VII
E_{total} (eV)	-185522.1821	-185522.1207	-185520.4137	-185520.3768	-185520.1417	-185519.3589	-185519.4791
$E_{binding}$ (eV)	-5.0099	-4.9485	-3.2415	-3.2046	-2.9695	-2.1867	-2.3069

Table 4.4
Cu (111) surface and L-glutamine total energies

$E_{surface}$ (eV)	-182737.4003
E_{glut} (eV)	-2779.7719

Interestingly, the energetically favored configuration is the on top site of L-glutamine along the [110] site, having the N and O atoms on top of Cu atoms as shown in Figure [5].

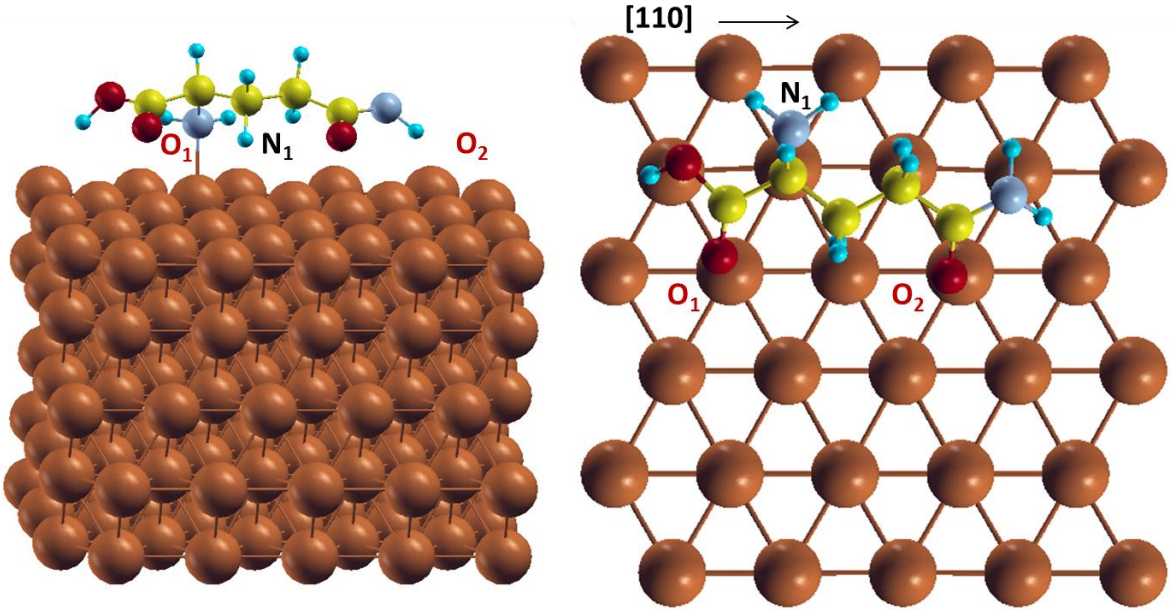

Figure [4.5]: On top site along the [110] site: (a) side view, (b) on top view. Energetically favored configuration of L-glutamine having the N and O atoms "on top" of Cu atoms. Grey, yellow, red, blue and orange balls stand for the N, C, O, H and Cu atoms, respectively.

4.2.2 Electronic properties

We continued our calculations with the energetically favored configuration and we investigated the electronic structure of the L-glutamine on Cu (111) surface. Figure [4.6] shows the total electronic density of states (EDOS). The Fermi energy is set to zero.

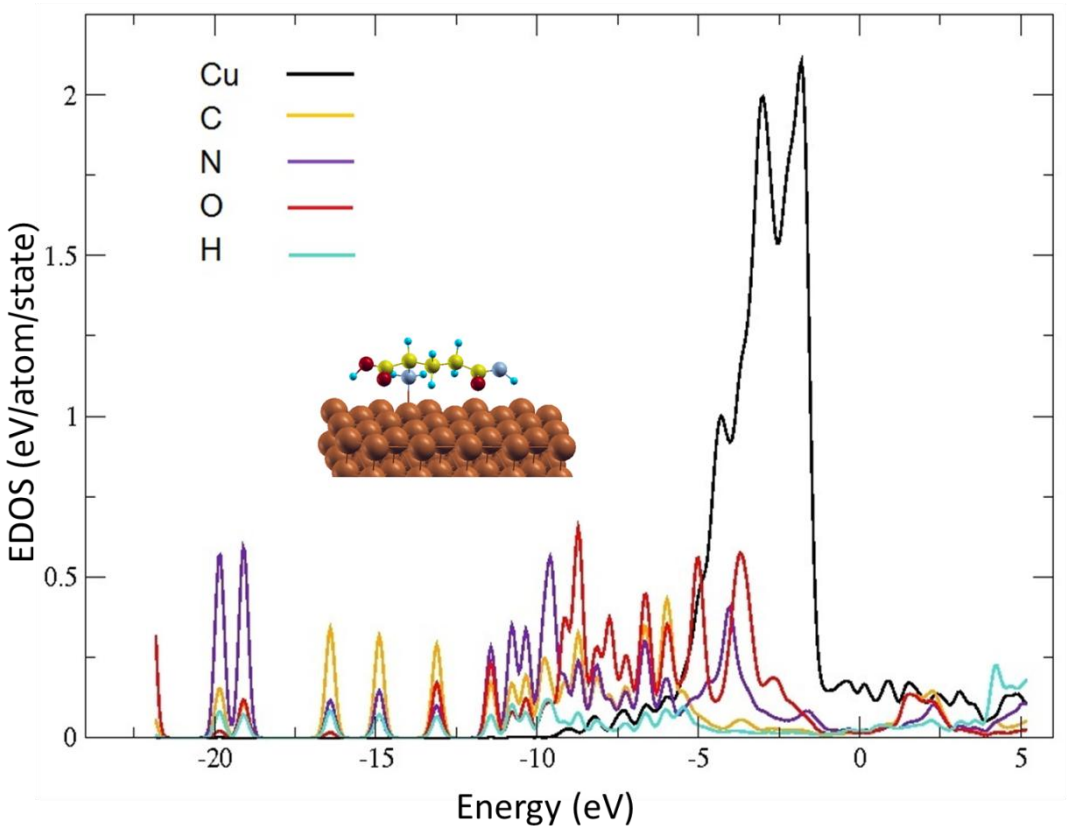

Figure [4.6]: Electronic density of states of L-glutamine and Cu (111) surface. Zero energy stands for the Fermi level. Black, orange, purple, red and blue lines stand for the Cu, C, N, O and H atoms, respectively.

The Cu electrons' states are shown to be more responsible for the occupation around the fermi level. In addition, we observe a main peak at the energy range from -1eV to -5 eV, which is in agreement with the bulk Cu's behavior [30]. The lower energy states are mainly due to L-glutamine's electrons. More specifically the EDOS along the energy

range from -5eV to -12 eV is mainly composed from the L-glutamine's N, O and C atoms while the H atoms show smaller contribution. In the energy range from -3.5 eV to -9 eV the EDOS reveals both surface atoms' and the amino acid's electron states indicating the existence of hybridizations. Finally, the density of states around -13 eV, -15 eV, -17eV and -20 eV are due to L-glutamine's atoms.

By projecting the wavefunction onto the s, p, d orbitals for each species of atoms separately, we present the partial density of states (PDOS) of the system in Figure [7], in order to study which type of electrons are the mainly responsible in each energy state and reveal the type of L-glutamine's bonding with the surface. In Figure [7] the total density of states for each type of atom of the system and the contribution of *s, p, d* orbital of Cu, *s, p* of C, O and N and *s* orbital of H atoms are presented.

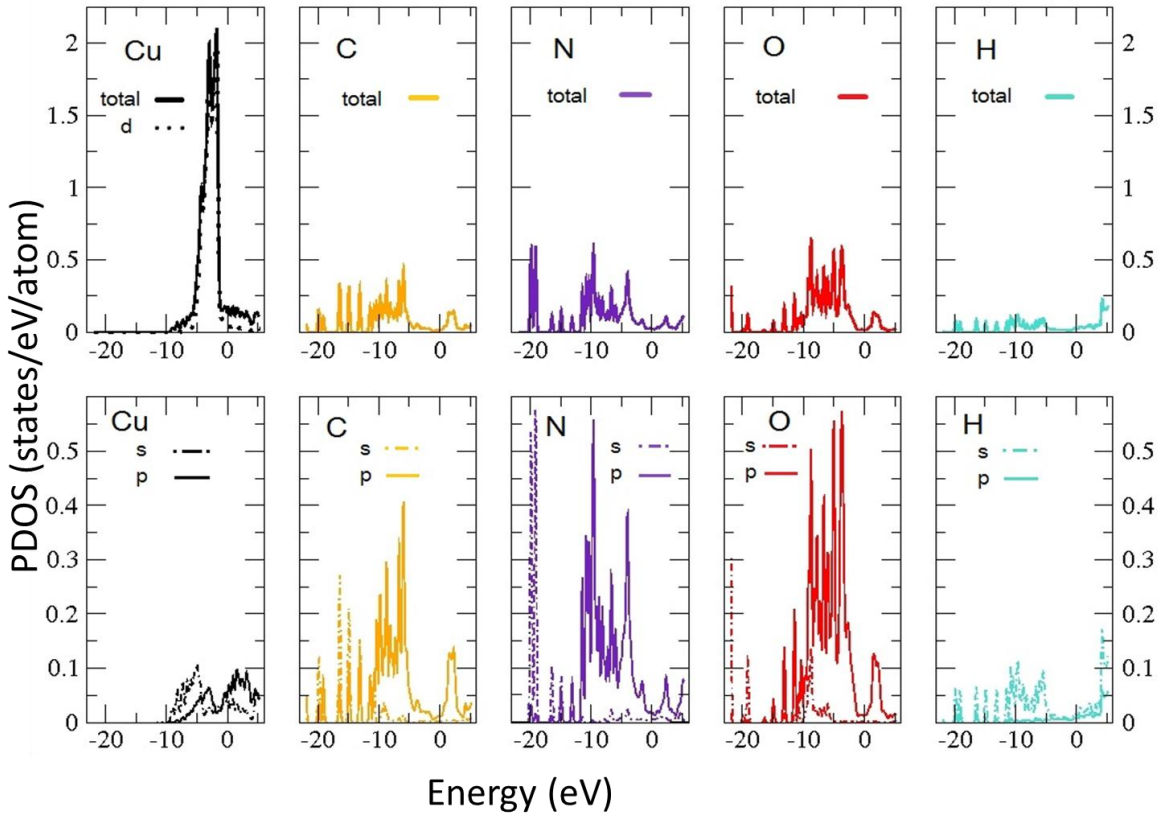

Figure [4.7]: Projected Electronic density of states of L-glutamine and Cu (111). Zero energy stands for the Fermi level. Solid thick lines stand for total, dotted for d orbitals of Cu, dot-dash lines for s orbitals and thin lines for p orbitals. Black, orange, purple, red and blue lines stand for the Cu, C, N, O and H atoms, respectively.

From the PDOS we can observe that Copper's *d* electrons contribute mostly in Fermi level state and *p* electrons of C, N and O are mainly responsible in lower energy states. Specifically in the range of -2 eV to -10 eV the *p* electrons of N, C, O have higher contribution. For all energies, the Hydrogen's *s* electron occupation is smaller than the other atoms. The higher contribution of N, C, O *p* orbital indicate the ability of these functional groups to form bonds with the surface, that theoretically has proved for the iron surfaces [20]. For this reason we expect to find bonded states in lower energies than Fermi level and especially in the energy range from -2.5 eV to -6 eV where surface's electrons and L-glutamine's electrons have some contribution.

In order to confirm these predictions we plotted selective wavefunctions. Figure [8] shows the wavefunction of the system (L-glutamine and Cu surface) close to the Fermi level where 8(a) shows the geometrically optimized structure and 8(b) and 8(c) show the optimized wavefunctions of E_{HOMO} and E_{LUMO} for the L-glutamine on Cu (111) surface, respectively.

The optimized electronic structures of L-glutamine on Cu (111) surface reveals that the Cu's *d* electrons contribute mostly around the Fermi level while the L-glutamine's orbitals have smaller contribution and indicating absence of bonding hybridization. It is remarkable that the surface electronic features are directly affected showing localization of the Cu's *d* orbital in the L-glutamine's neighborhood. Figure [4.8] also shows weak hybridizations where H atoms also participate that are formed between the molecule and the surface close to the Fermi level state while at lower energy states such hybridizations were not observed. Several experimental studies have shown that amino acids on Cu surfaces can form Hydrogen bonds with metal atoms once the parallel orientation of the molecule has its carboxylate group and the amino group towards the surface [31]. It should be noted that our favored configuration is in agreement with these studies as the amino acid L-glutamine has both its sidechain and backbone lied down on the Cu (111) surface.

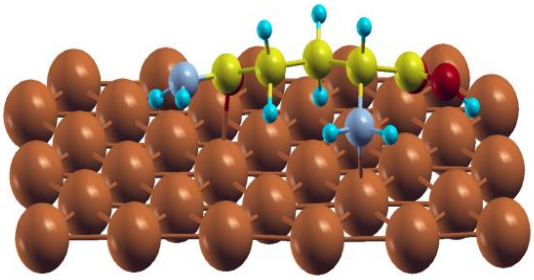

(a) optimized structure

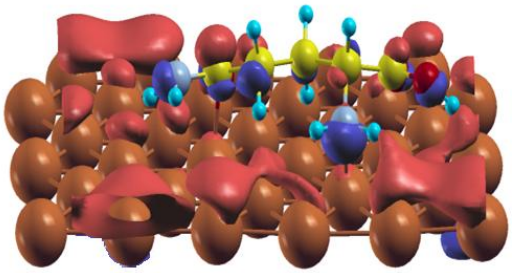

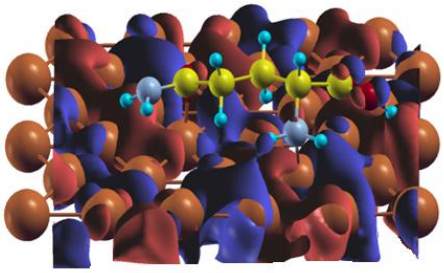

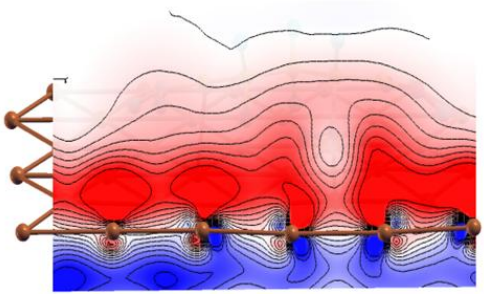

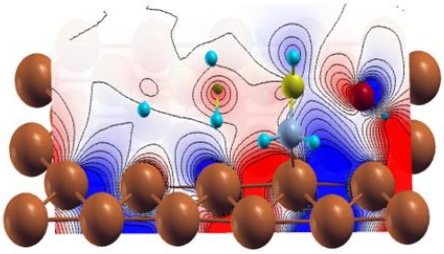

(b) HOMO

(c) LUMO

Figure [4.8]: Electronic properties of L-glutamine and Cu (111) surface. Red and blue colours indicate particular isosurfaces at positive and negative values, respectively. (a) optimized structure, (b)optimized systems' wavefunctions in E_{HOMO} and (c) in E_{LUMO}.

Furthermore, we studied selective wavefunctions at ~~for~~ lower energy states far from the Fermi level. In Figure [4.9] we present the wavefunctions for the energy states: E= -3.7541 eV, E= -4.9941 eV and E= -5.0341 eV. The choice of these energies was made according to the common electron occupation of the L-glutamine's and Copper's states in the EDOS graph and their visible charge density contribution in the corresponding wavefunction.

(a) WF at -3.7541 eV (b) WF at -4.9941 eV (c) WF at -5.0341 eV

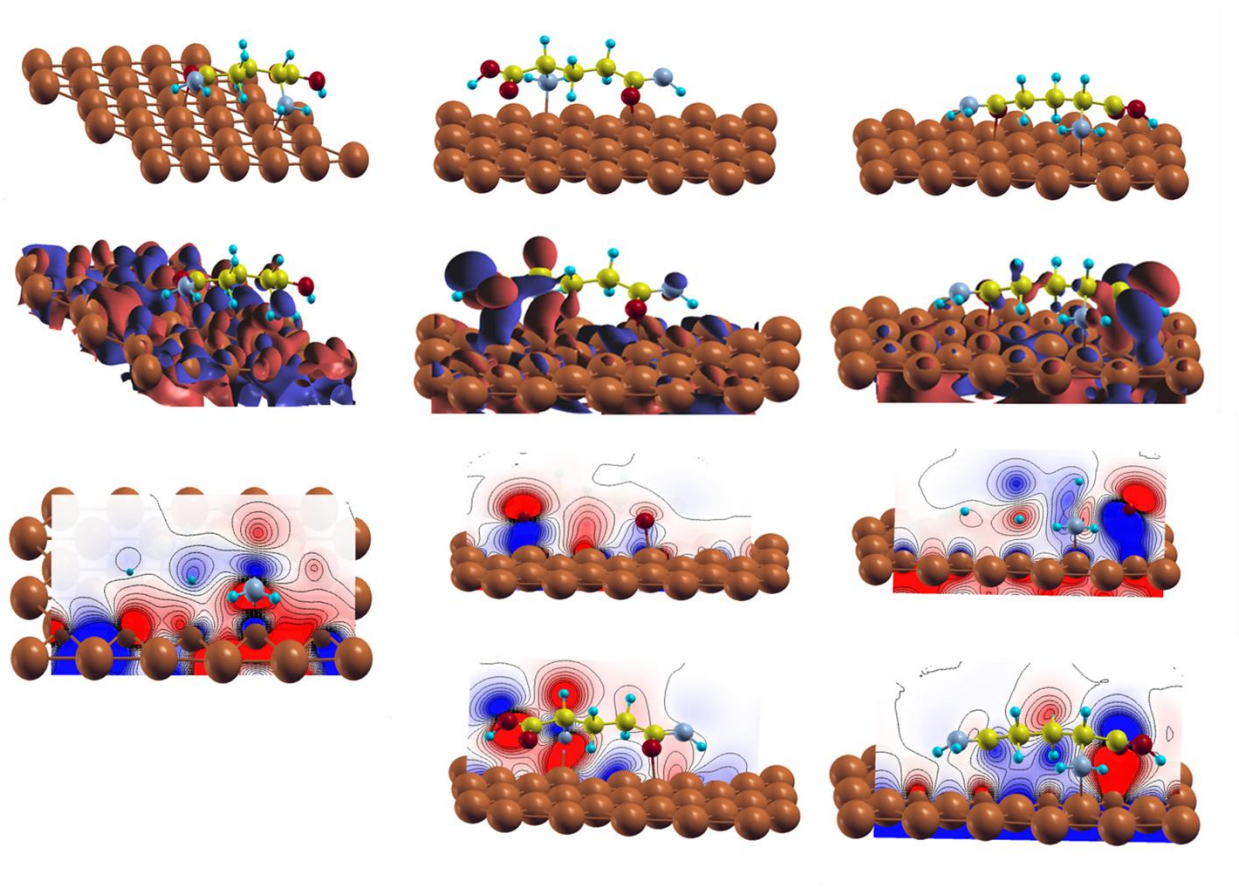

Figure [4.9]: Optimized L-glutamine / Cu (111) system's wavefunctions at (a) E= -3.7541 eV, (b) E= -4.9941 eV and (c) -5.0341 eV. Grey, yellow, red, blue and orange balls stand for the N, C, O, H and Cu atoms, respectively.

Figure [4.9] shows that L-glutamine's N and O atoms form bonded states with Copper's atoms. This is explained by the presence of vacant d orbital lobes of the Cu surface atoms that form coordinate bonds with atoms able to donate electrons. In figure (a) we can see that L-glutamine forms bond through the backbone's N atom. We also observe in figure (b) and (c) that there are hybridizations via two different functional groups of L-glutamine on Cu (111) surface. Nitrogen's and Oxygen's p orbitals are hybridized with Copper's d electrons. That is in excellent agreement with the behavior of L-glutamine and other Nitrogen containing organic compounds adsorbed on metallic surfaces [20], [6], [26].

4.3 TWO L-GLUTAMINES ON CU (111) SURFACE

Since the L-glutamine can adsorb on Cu (111) surface through its functional groups N and O we continued our DFT calculations similarly depositing two molecules that interact and almost cover the computational surface layer creating in this way an organic coating. Choosing the energetically favored configuration of L-glutamine having the N and O atoms "on top" of Cu atoms, we deposited the two molecules aligned parallel or antiparallel as shown in Figure [4.10]. The system's energy was minimized until the forces between the atoms were less than 0.5 eV/Å.

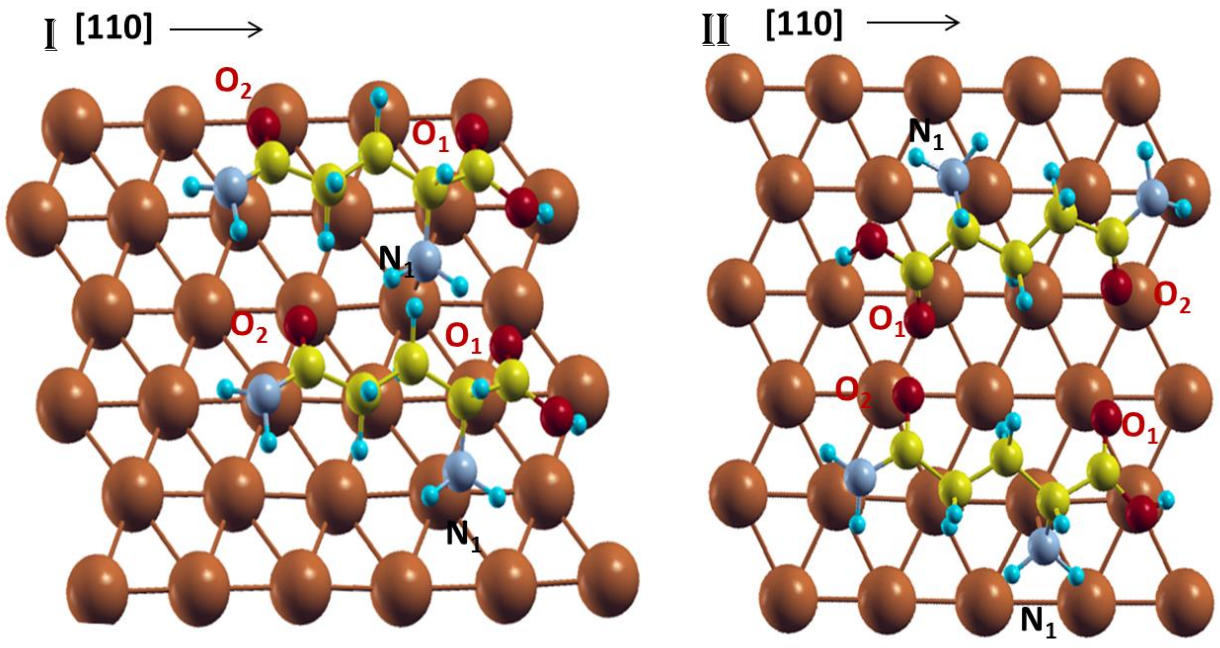

Figure [4.10]: Configurations of two molecules on Cu (111) surface: **(**I) Parallel aligned L-glutamines "on top" of Cu (111) surface (II) Antiparallel L-glutamines on Cu (111) surface. Grey, yellow, red, blue and orange balls stand for the N, C, O, H and Cu atoms, respectively.

Based on the optimized configurations, the binding energy of adsorption between the two L-glutamines on the Cu surface was calculated using the following equation:

$$E_{binding} = \frac{E_{total} - E_{surface} - nE_{glut}}{n} \quad (4.2)$$

where n is the number of molecules (in our case n=2), E_{total} is the total energy of the Cu surface - L-glutamines system, $E_{surface}$ is the total energy of the Cu surface and E_{glut} is the total energy of the L-glutamine molecule. The values of the total and binding energies are listed in Table [5].

Table 4.5

Total and binding energies of the molecules of L-glutamine on Cu (111) surface for the two different configurations .

Configurations	I (parallel)	II (antiparallel)
E_{total} (eV)	-188305.7667	-188301.0348
$E_{binding}$ (eV)	-4.4113	-2.04535

Table 5 shows that, after the energy was minimized, the binding energy of the configuration I is lower than the configuration's ii, so we conclude that the energetically favored configuration of the two L-glutamines on Cu (111) surface stands for the parallel aligned molecules. We continued our calculations with the energetically favored configuration and we present the corresponding total electronic density of states (EDOS) having the Fermi energy at zero in Figure [4.11].

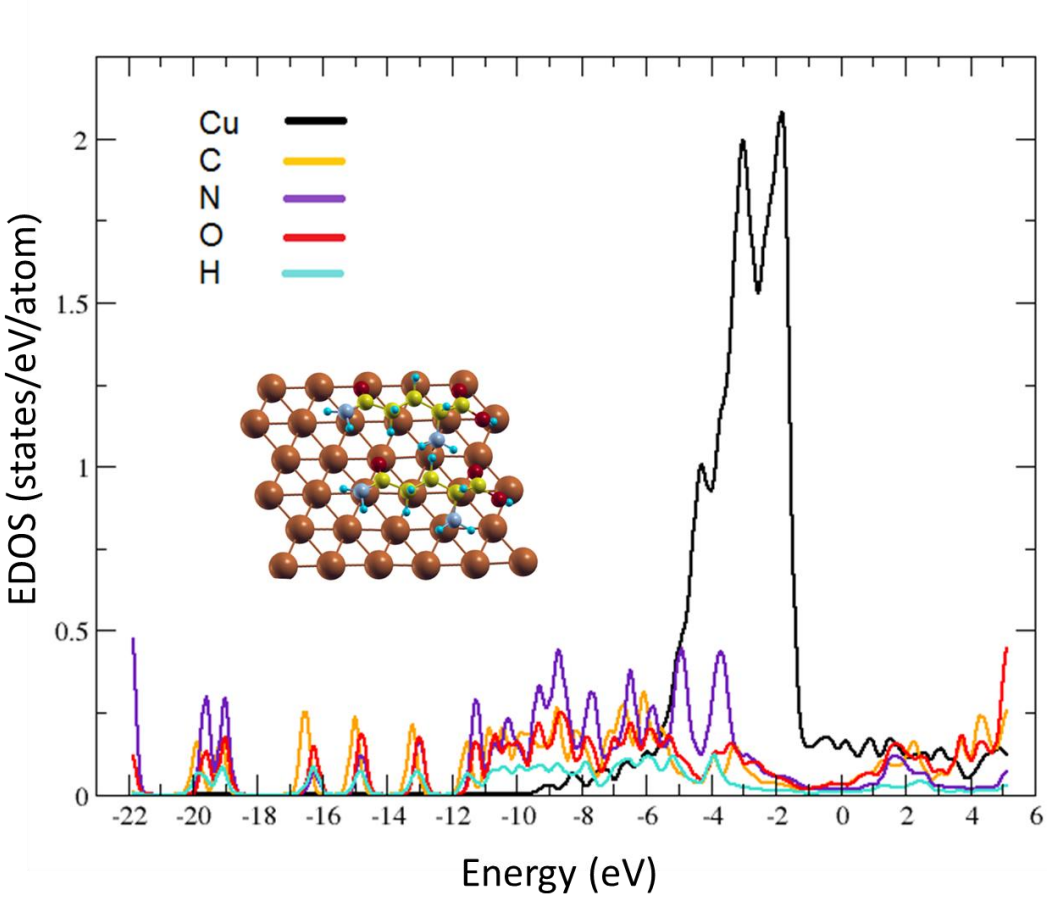

Figure [4.11]: Electronic density of states of two L-glutamines on Cu (111) surface. Zero energy stands for the Fermi level. Black, orange, purple, red and blue lines stand for the Cu, C, N, O and H atoms, respectively.

The EDOS shows similar behavior with the adsorption of one L-glutamine on Cu (111) surface. In particular, Copper's electrons are more responsible for the fermi level states while in lower energy states the L-glutamines' atoms mainly contribute, similarly to the single case. Moreover, all atoms contribute to the energy states from -3.5 eV to -9 eV. The EDOS peaks of the two L-glutamines on Cu are lower and wider compared to the one L-glutamine case indicating intermolecular interactions. In the EDOS of one L-glutamine we observe highest contribution of Oxygen atoms following by the Nitrogen and the Carbon while in the two L-glutamine's case, Nitrogen reveals the major contribution. In addition, although all heteroatom's peaks are lower compared to the single case, Nitrogen has higher peak than Oxygen which means higher contribution. This behavior can be explained by the presence of the hydrogen intermolecular bond where Nitrogen atoms of the second L-glutamine participate.

In order to study further the contribution of C, N, O, H orbitals and surface's Cu orbitals, we plotted in Figure [4.12] the projected density of states (PDOS).

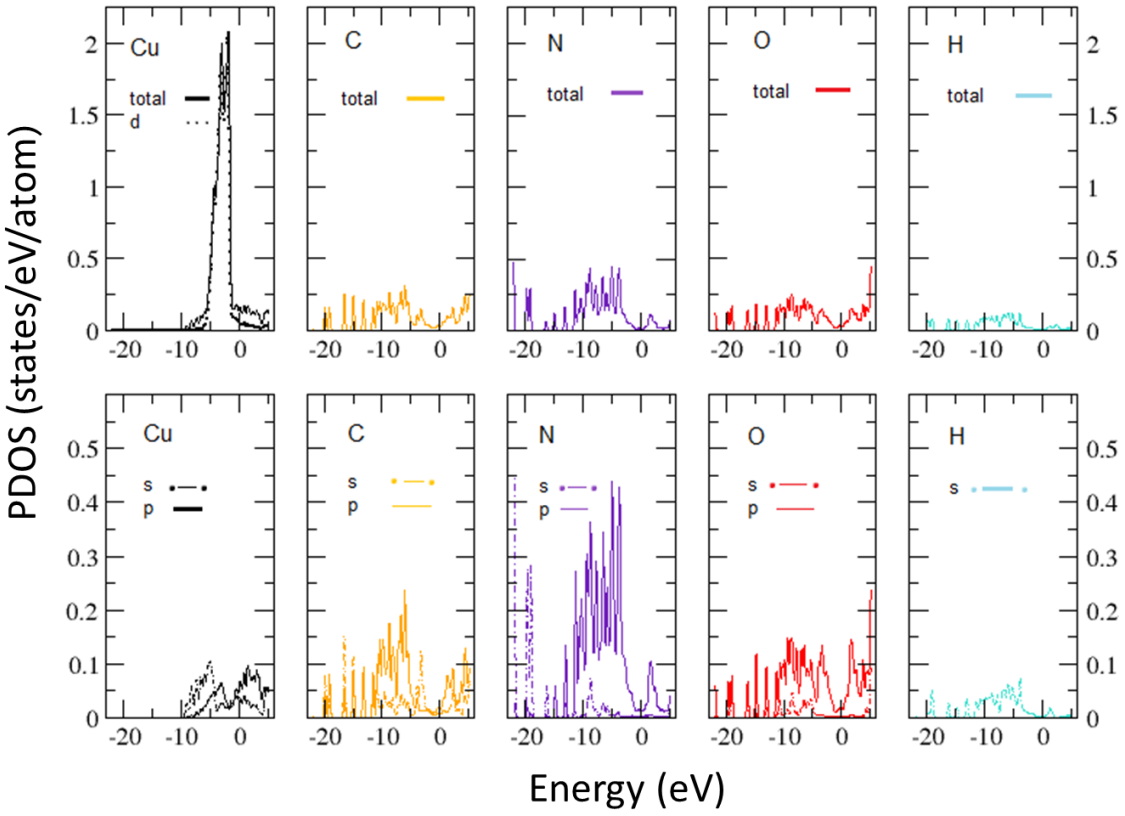

Figure [4.12]: Projected Electronic density of states of two L-glutamines and Cu (111). Zero energy stands for the Fermi level. Solid thick lines stand for total, dotted for d orbitals of Cu, dot-dash lines for s orbitals and thin lines for p orbitals. Black, orange, purple, red and blue lines stand for the Cu, C, N, O and H atoms, respectively.

In Figure [4.12], we observe that Cu's *d* electrons are responsible for the Fermi level states while L-glutamines' electrons contribute more at lower energies in line with the single case. This means that the presence of the second L-glutamine did not change the fermi level states. In addition there is no difference in the behavior of s, p orbitals of Copper's atoms. Moreover, we observe also that N's, C's and O's orbitals are more responsible for the energy states below -2.0eV. PDOS graph confirms that Nitrogen's p orbitals have higher contribution than Carbon and Oxygen. The Hydrogen's s orbitals have very low contribution similarly to the one molecule's case. The maximum of Nitrogen's density of states reaches almost 0.45

(states/eV/atom), in contrast with the study of the one L-glutamine on Cu (111) surface where the maximum was around 0.6 (states/eV/atom). The Oxygen's and Carbon's orbitals have same behavior as the density of states for Oxygen's p electrons reaches almost 0.15 (states/eV/atom) in the two molecules system and 0.55 (states/eV/atom) in the one molecule system. The density of states for Carbon's p electrons reaches 0.25 (states/eV/atom) in the two molecules system and 0.40 (states/eV/atom) in the one molecule system. Finally, the s electrons of N, O, C atoms show small differences between the single and the double L glutamine's cases.

For a better interpretation of the EDOS conclusions we optimized the system's wavefunctions around the Fermi level as shown in Figure [4.13]. Figure 4.13(a) shows the optimized structure, Figures 4.13(b) and 4.13(c) show the optimized HOMO and LUMO wavefunctions of the two L-glutamine's molecules on Cu (111) surface, respectively.

Figure [4.13] reveals that Copper's *d* electrons are responsible for the Fermi level states while the L-glutamines' orbitals contribute less in both HOMO and LUMO. We observe similar behavior with the one L-glutamine suggesting that Cu (111) surface is also affected by the presence of the two amino acids showing the Cu- *d* orbitals spotted around the two L-glutamines. In both E_{HOMO} and E_{LUMO} states there are anti-bonding hybridizations between the molecules and the metallic surface.

It should be noted that around the Fermi level we observe hybridizations where H atoms participate similarly to the one molecule case. This could be explained by the fact that the two molecules have been deposited, again, on top of the surface with both their sidechain and backbone lied down on the Cu (111) surface.

(a) optimized structure

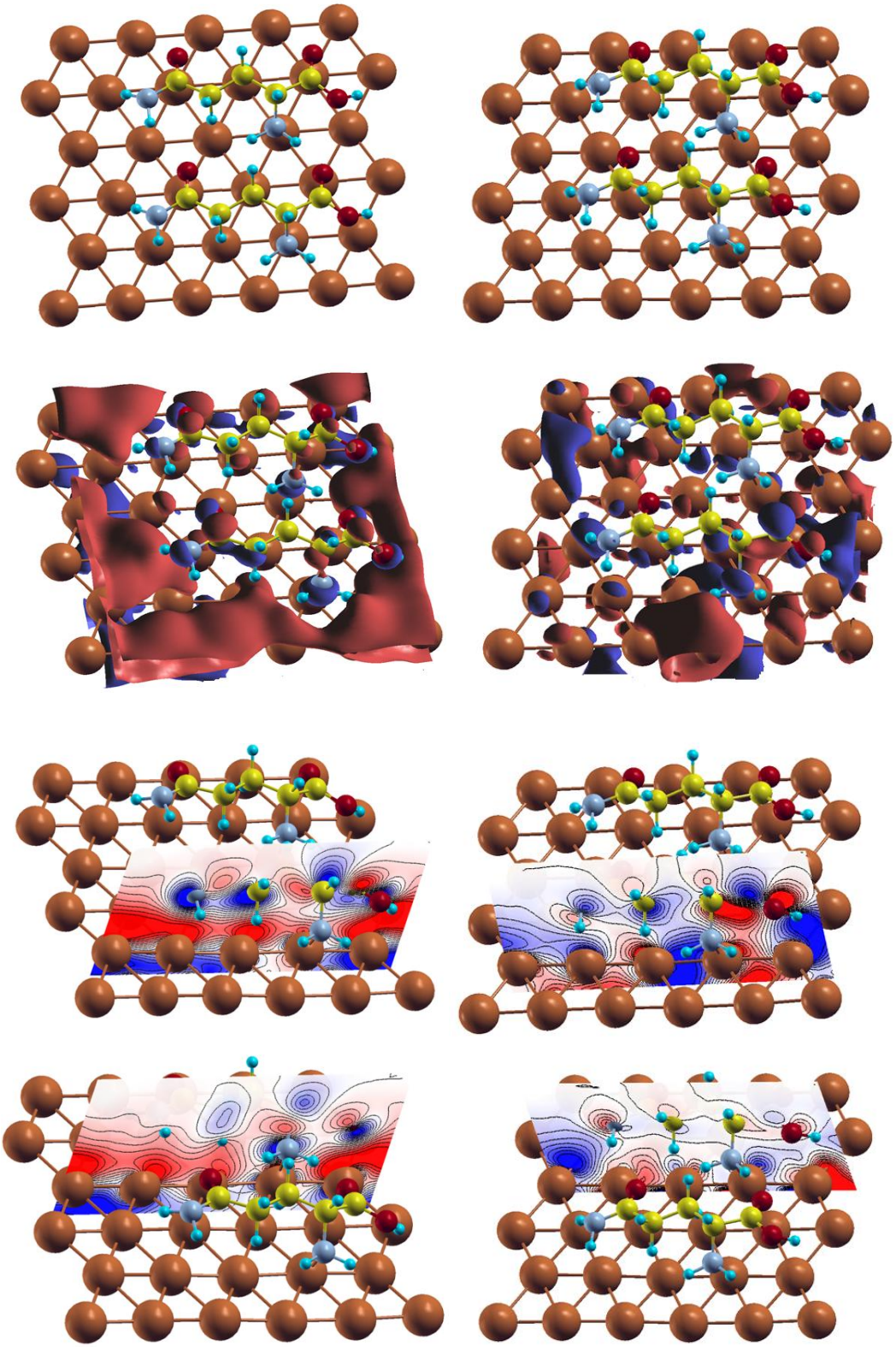

(b) HOMO

(c) LUMO

Figure [4.13]: Electronic properties of two L-glutamines and Cu (111) surface. Red and blue colours indicate particular isosurfaces at positive and negative values, respectively. (a) optimized structure and optimized systems' wavefunctions in (b) E_{HOMO} and (c) in E_{LUMO}.

From the EDOS and PDOS we expect that L-glutamines may form bonded states with the Cu (111) surface far from the Fermi level. In Figure [14] we present the optimized wavefunctions for selective energy states: E= -3.69561 eV, E= -3.94885 eV, E= -5.28743 eV and E= - 5.75773 eV

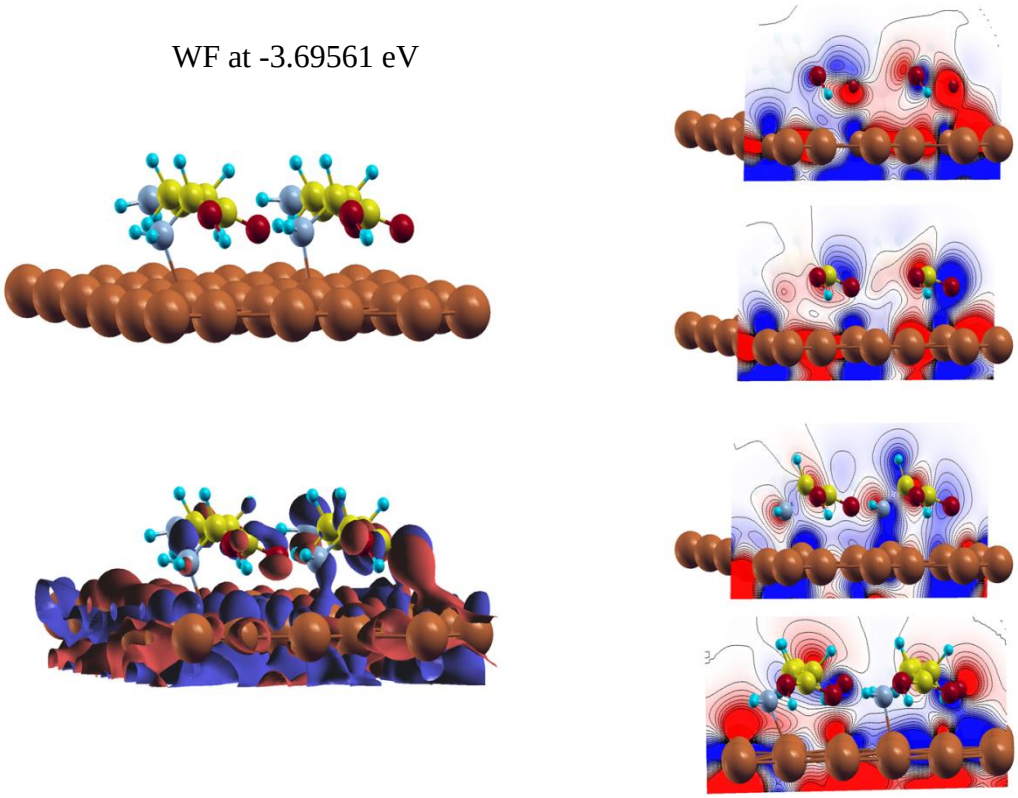

Figure [4. 14]: Optimized two L-glutamines / Cu (111) system's wavefunctions at E= -3.69561 eV. Grey, yellow, red, blue and orange balls stand for the N, C, O, H and Cu atoms, respectively.

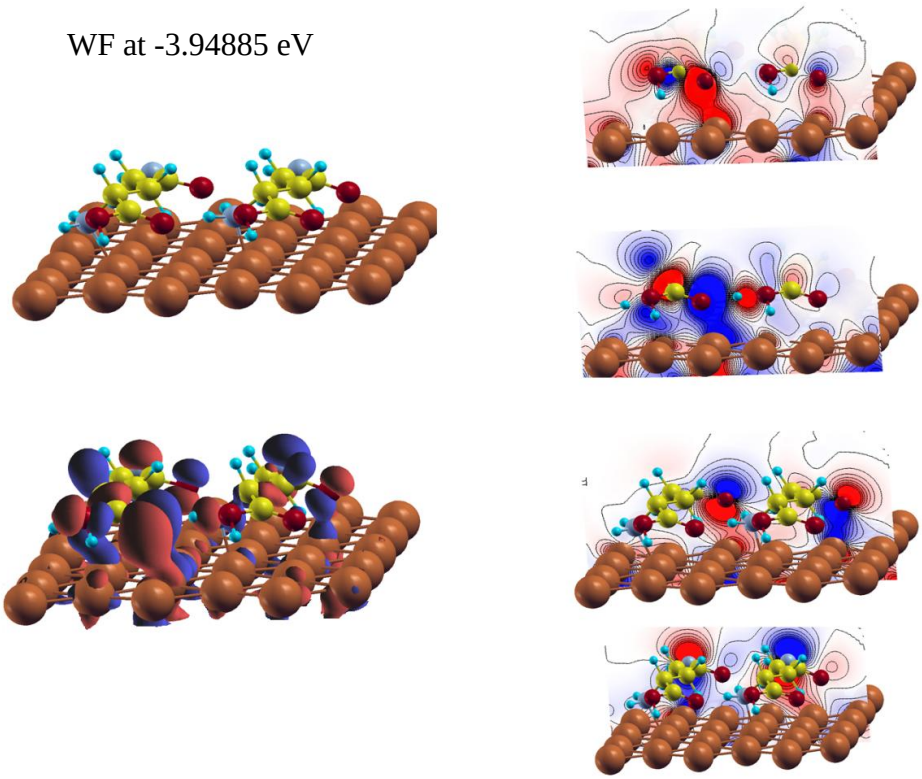

Figure [4.15]: Optimized two L-glutamines / Cu (111) system's wavefunctions at E= -3.94885 eV Grey, yellow, red, blue and orange balls stand for the N, C, O, H and Cu atoms, respectively.

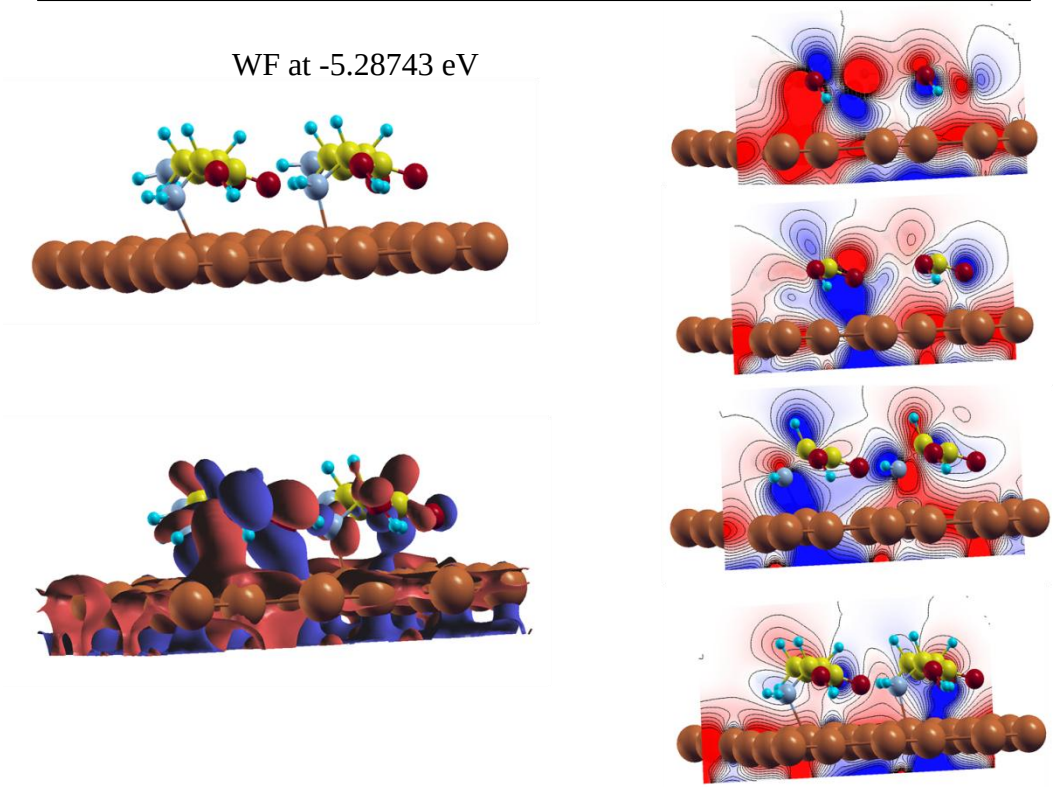

Figure [4.16]: Optimized two L-glutamines / Cu (111) system's wavefunctions at E= -5.28743 eV. Grey, yellow, red, blue and orange balls stand for the N, C, O, H and Cu atoms, respectively.

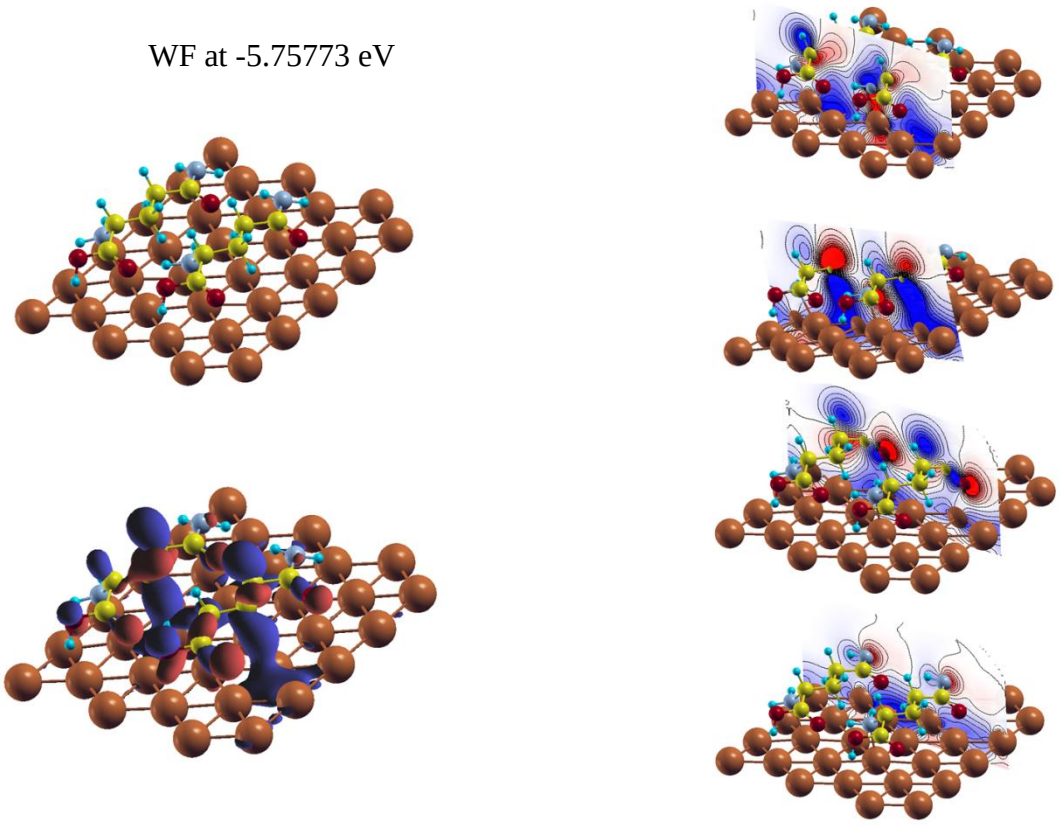

Figure [4.17]: Optimized two L-glutamines / Cu (111) system's wavefunctions at E= -5.75773 eV. Grey, yellow, red, blue and orange balls stand for the N, C, O, H and Cu atoms, respectively.

In Figure [4.14-4.17] we observe that the L-glutamines form bonds with the surface's atoms at several energies. As we expected, these bonds are formed by the functional groups of L-glutamine N, O and C while another general observation is that both L-glutamine molecules participate in these hybridizations.

More specifically Figure 4.14 reveals that the one molecule of L-glutamine contributes more in the bonding at the -3.69561 eV. Backbone Nitrogen and Oxygen atoms form bonds with Cu's atoms. In Figure 4.15 we observe that both L-glutamine molecules create bonds using their Oxygen atoms. Moreover, we observe bonding hybrizations between the O's p orbitals and Cu's d orbitals. In Figure 16 we can see that at -5.28743 eV one molecule of L-glutamine forms bonds with the Nitrogen and Oxygen atoms of its backbone and the other molecule forms bonds with the Nitrogen of its sidechain. Finally,

Figure 4.17 shows similar behavior with the other wavefunctions as the Oxygen atoms forms bonded states. In comparison with the other energy states we observe that Carbon atom of both molecules form bonds with the surface's atoms something that was not so clear in the one molecule case. In literature some organic compounds were expected to form coordinate bonds with the Fe surface's atoms through their Carbon atoms [26]. In addition to this, it is mentioned in literature that the –C=O carbonyl group is operative in a back-donation process for the Cysteine deposited on Cu (111) surface [10]. Furthermore in Figure 4.14d the two L-glutamines present similar charge distribution in this energy state while in the other energy states the electron behavior between the two molecules is different.

In conclusion we observe that the two molecules form bonded states with the Cu (111) surface's atoms at various energies while in general they present a similar behavior with the single L-glutamine. The design of a coat of L-glutamine molecules on the surface could be successful. It is interesting to present how the second L-glutamine molecule affects the behavior

5 MOLECULAR DYNAMICS SIMULATIONS

5.1 INTRODUCTION OF MOLECULAR DYNAMICS SIMULATION

One of the principal tools in the theoretical study of biological molecules is the method of molecular dynamics simulations (MD). This computational method calculates the time dependent behavior of a molecular system. MD simulations have provided detailed information on the fluctuations and conformational changes of proteins and nucleic acids. Beginning in theoretical physics, the method of MD gained popularity in materials science and since the 1970s also in biochemistry and biophysics. These methods are now routinely used to investigate the structure, dynamics and thermodynamics of biological molecules and their complexes. They are also used in the determination of structures from X-ray crystallography and from NMR experiments. Molecular dynamics simulations permit the study of complex, dynamic processes that occur in biological systems [35].

Molecular Dynamics (MD) simulation was performed in this study by means of the SIESTA code.

In the present study, MD calculations were performed on some characteristic configurations in order to research the organic molecules' adsorption configuration and the ability of creation organic coatings on metallic surfaces.

5.2 Theory of MD

In Molecular Dynamics simulation, the evolution of the positions and velocities of the atoms with time are calculated solving Newton's equations of motion:

$$F = -\frac{\partial E}{\partial x} = ma = m\frac{\partial^2 x}{\partial t^2} \tag{5.1}$$

First step in every MD simulation is the definition of the initial coordinates of the atoms. The electrons are treated quantum mechanically and the nuclei classically.

Based on an initial set of positions, velocities and accelerations, the equations of motion are solved numerically in discrete time steps. The time must be small enough to accurately sample highest frequency motion.

Integration of the equations of motion yields a trajectory that describes the positions, velocities and accelerations of the particles as they vary with time. The method is deterministic; once the positions and velocities of each atom are known, the state of the system can be predicted at any time in the future or the past.

5.2.1 Verlet Algorithm

. Verlet integration is a numerical method used to integrate Newton's equations of motion and the system is assumed as micro canonical, which means that the number of atoms, the volume and the energy are stable (NVE). The Verlet algorithm is the most commonly used algorithm in Molecular Dynamics simulation.

All the integration algorithms assume the positions, velocities and accelerations can be approximated by a Taylor series expansion:

$$r(t+\delta t) = r(t) + v(t)\delta t + \frac{1}{2}a(t)\delta t^2 + \ldots$$

$$v(t+\delta t) = v(t) + a(t)\delta t + \frac{1}{2}b(t)\delta t^2 + \ldots$$

$$a(t+\delta t) = a(t) + b(t)\delta t + \ldots \qquad (5.2)$$

Where ***r*** is the position, ***v*** is the velocity (the first derivative with respect to time), ***a*** is the acceleration (the second derivative with respect to time), etc.

To derive the **Verlet** algorithm one can write

$$r(t+\delta t) = r(t) + v(t)\delta t + \frac{1}{2}a(t)\delta t^2$$

$$r(t-\delta t) = r(t) - v(t)\delta t + \frac{1}{2}a(t)\delta t^2$$

Summing these two equations: $$r(t+\delta t) = 2r(t) - r(t-\delta t) + a(t)\delta t^2 \quad (5.3)$$

The Verlet algorithm uses positions and accelerations at time *t* and the positions from time *t-dt* to calculate new positions at time *t+dt* [36], [37].

5.3 INPUT FILE FOR MD CALCULATIONS

The program has an outer geometry loop: it computes the electronic structure (and thus the forces and stresses) for a given geometry, updates the atomic positions (and maybe the cell vectors) accordingly and moves on to the next cycle.

Several options for MD and structural optimizations are implemented, selected by MD.TypeOfRun. In our calculations the Verlet algorithm has been used.

During the molecular dynamics type of run, the program moves the atoms (and optionally the cell vectors) in response to the forces (and stresses), using the classical equations of motion. The atoms are assigned random velocities drawn from the Maxwell-Bolzmann distribution with the corresponding temperature.

The difference in the FDF file is the commands for MD simulation that must be inserted. The initial and the final time step, the length of time step and the initial temperature is defined in the input (fdf) file as shown in Figure [5.1].

```
MD.TypeOfRun            Verlet          # Type of dynamics:
MD.LengthTimeStep       1.0 fs        # Type of dynamics:
MD.InitialTimeStep      1           # Type of dynamics:
MD.FinalTimeStep        1000          # Type of dynamics:
MD.InitialTemperature   600.0 K    # Type of dynamics:
```

Figure [5.1]: Input commands for MD calculations

As presented in Figure [5.1], the initial temperature was set at 600 K and the length of the time step at 1.0 fs in our calculations. The amount of the total steps of the MD simulation is different in every studied case depending on the systems' behavior.

Every command that is not needed in FDF file is turned into a comment with a hush mark at the beginning.

5.4 RESULTS AND DISCUSSION

We performed Molecular Dynamics simulations, in order to study the preferred adsorption orientation of L-glutamine on Cu (111) surface. We started using the relaxed configurations of L-glutamine on Cu surface.

The MD calculations performed in several different configurations as shown in Figure [5.2].

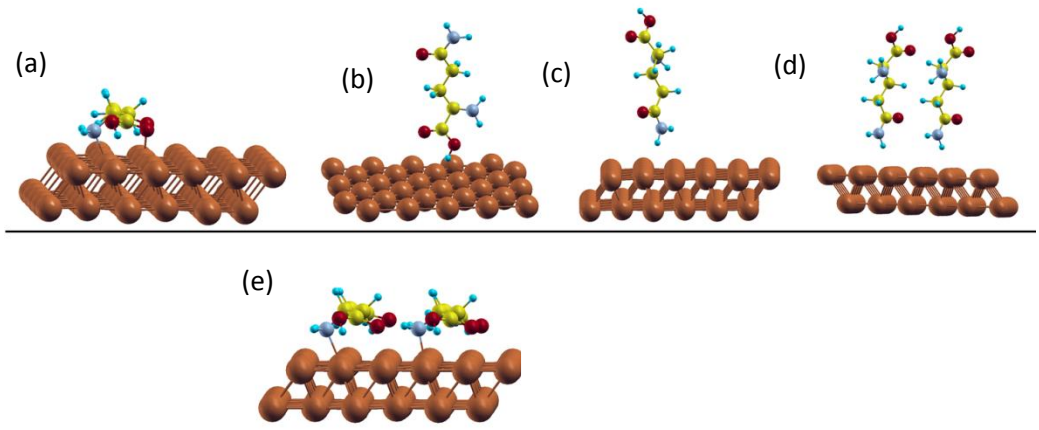

Figure [5.2]: Initial configurations of L-glutamine on Cu (111)

Figure [5.2] (a) shows the energetically favored configuration of the single L-glutamine on Cu (111) surface, which is the on top site along the [110] site having the N and O atoms "on top" of Cu atoms. Figure [5.2] (b) shows the vertical position of L-

glutamine molecule on Cu (111) layer with the O atom closer to the surface layer. Figure [5.2] (c) and (d) presents the vertical position of single L-glutamine on Cu (111) surface with the O atom closer to the surface and the vertical position of two molecules respectively. In Figure [5.2] (e) the energetically favored configuration of two L-glutamine molecules on Cu (111) surface is shown.

The initial configurations and representative snapshots showing the alterations in adsorption orientation of L-glutamine on Cu surface during the MD simulation are presented at the next figures.

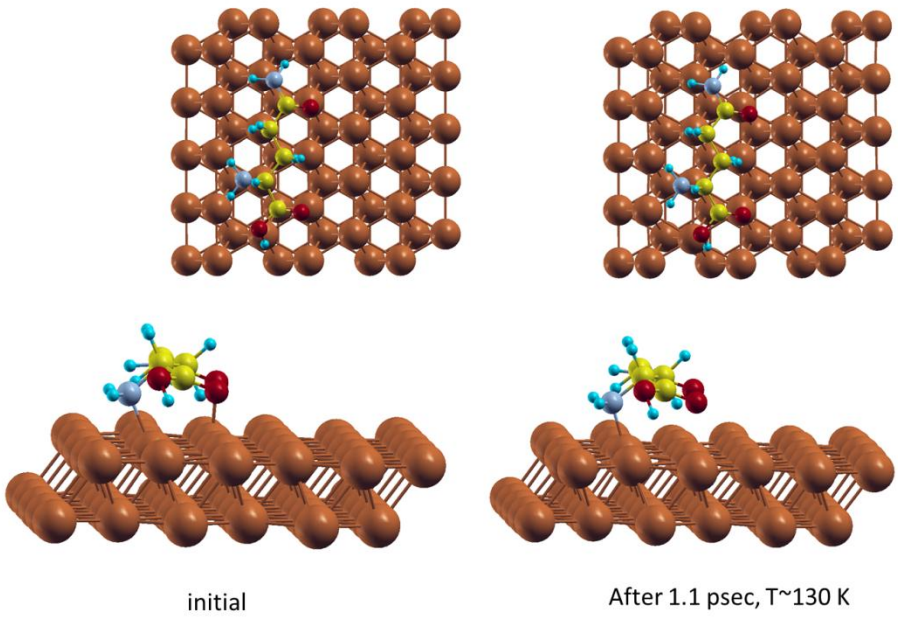

Figure [5.3]: Representative snapshots of L-glutamine on top site along the [110] site of Cu surface having the N and O atoms "on top" of Cu atoms showing changes in adsorption orientation during MD simulation

In Figure [5.3] we observe that the L-glutamine's Nitrogen and Oxygen are "on top" of Cu surface's atoms retain their positions and the orientation of L-glutamine has not shifted as the temperature is increased. The molecule maintains its structure as there is no spectacular difference at the positions of L-glutamine's atoms. The Oxygen and Nitrogen atoms are slightly shifted.

We notice similar behavior in the case where the two molecules of L-glutamine are aligned parallel “on top” of Cu (111) surface, Figure [5.4].

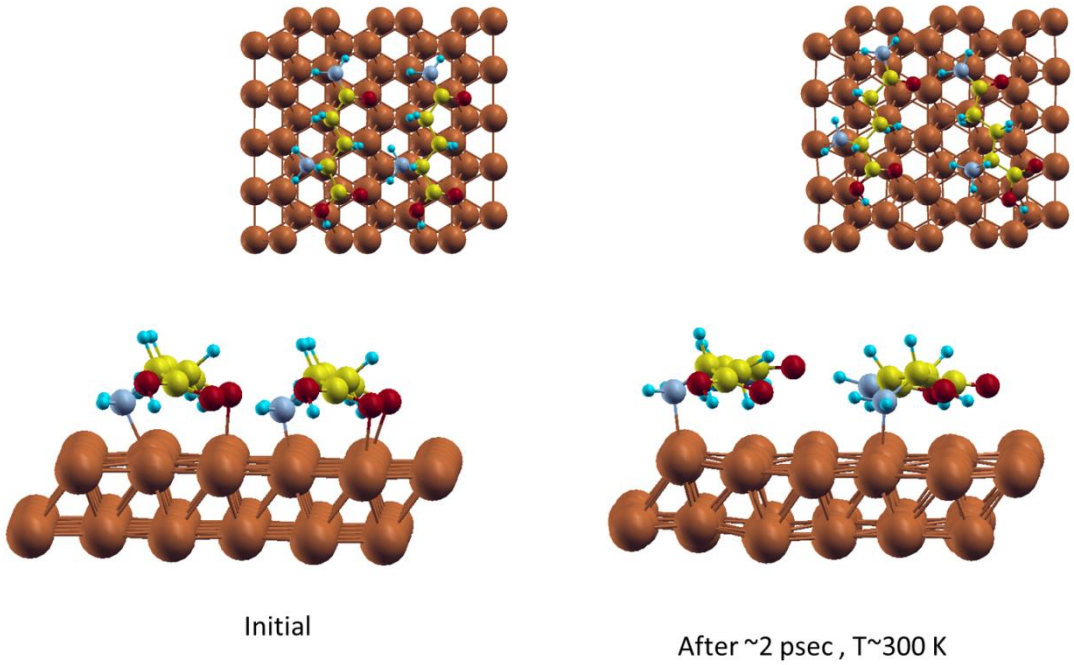

Figure [5.4]: Representative snapshots of two L-glutamine aligned on top of Cu atoms parallel to [110], showing changes in adsorption orientation during MD simulation

Figure [5.4] reveals that the orientation of the two L-glutamines is not changed through the MD simulation. The molecule’s atoms are slightly shifted. The L-glutamine’s Nitrogen and Oxygen atoms are not “on top” positions. This can be explained by the intermolecular interactions. Several studies have shown that amino acids interact by forming Hydrogen bonds.

Following, we performed MD simulation on the vertical deposited L-glutamine molecules on Cu (111) surface. Firstly, the molecule’s Oxygens are near the surface as shown in Figure [5.5] and secondly the molecule’s Nitrogen is toward the surface as shown in Figure [5.6].

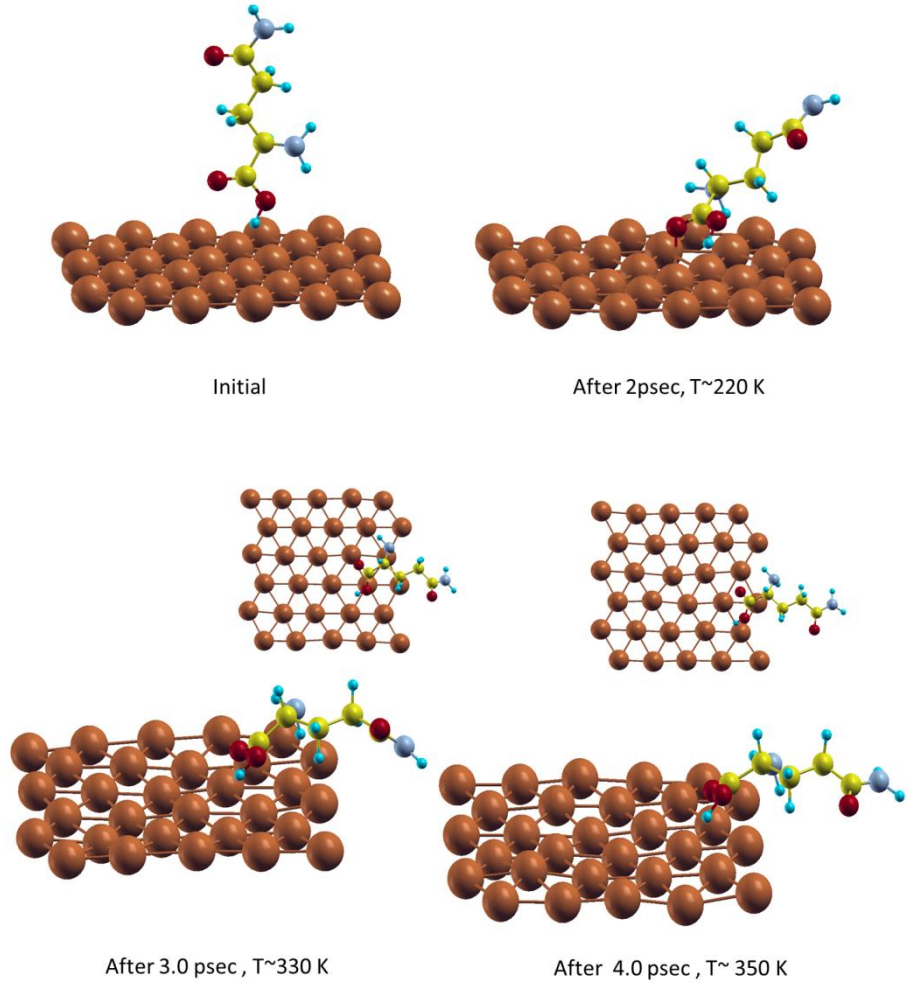

Figure [5.5]: Representative snapshots of L-glutamine vertical, with Oxygen atom above one layer of Cu (111) surface showing changes in adsorption orientation during MD simulation

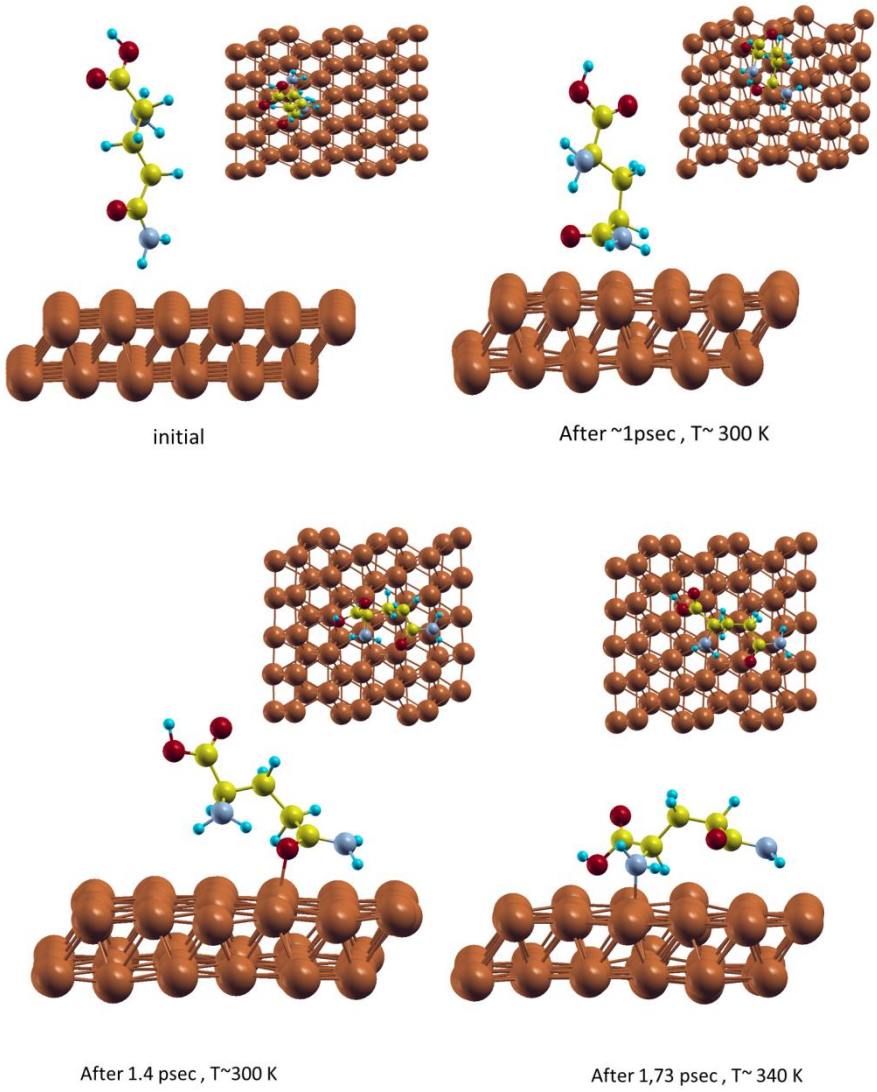

Figure [5.6]: Representative snapshots of L-glutamine vertical with Nitrogen atom above two layers of Cu (111) surface showing changes in adsorption orientation during MD simulation

The behavior of the vertical L-glutamine with the Nitrogen or the Oxygen atom above the metallic surfaces is really interesting. Figure [5.5] and [5.6] show that as the temperature increases the molecule falls onto the surface. Both configurations acquire only 1 psec or 2 psec to change their orientation. The L-glutamine's Nitrogen and Oxygen are towards the surface and the alkyl chain relaxes outwards. This behavior is explained by the ability of the functional groups (Nitrogen and Oxygen) of L-glutamine to form bonds with

the Cu (111) surface's atoms as have been proved by our DFT relaxed calculations (Chapter 4).This state is in agreement with several studies with MD simulation of organic molecules on metallic surfaces [26], [27]. We also notice that in the case where the L-glutamine's oxygen is above the surface (Figure [5]), the molecule "lies down" along the [110] of the surface as the energetically favored configuration. Furthermore, L-glutamine's Nitrogen and/or Oxygen are located "on top" of Cu atoms.

In addition, we performed MD simulation to study the behavior of two molecules vertical to the surface. We chose the energetically favored configuration of the vertical molecules, as the DFT calculation proved (Chapter 4.2.1, Table 3). Representative snapshots of the MD simulation are presented in Figure [5.7].

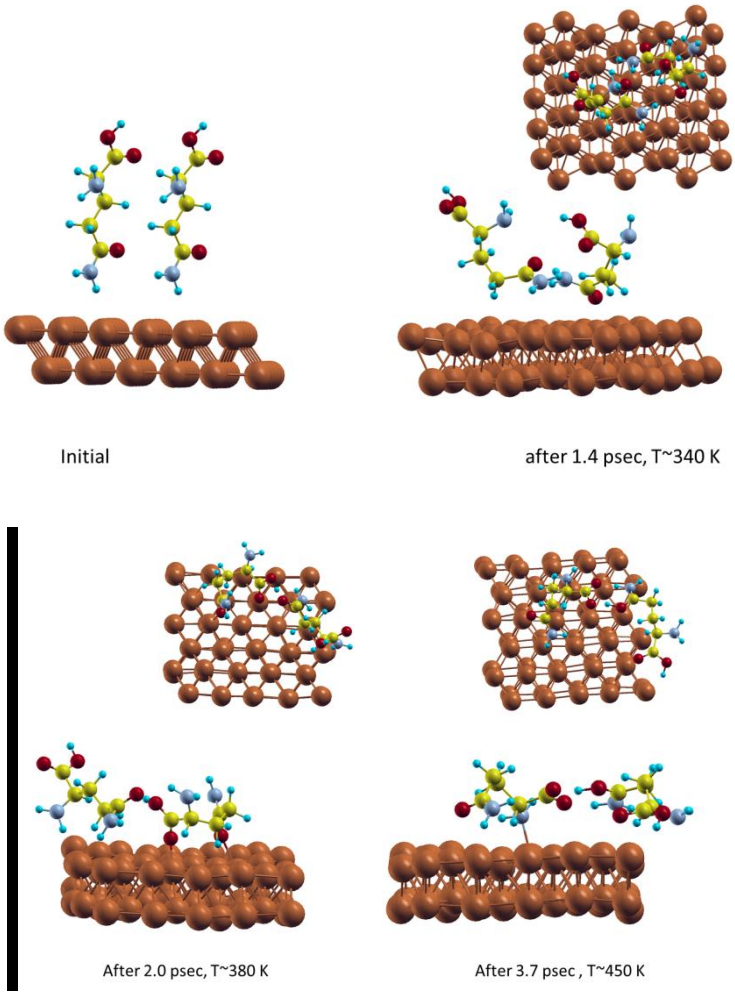

Figure [5.7]: Representative snapshots of two L-glutamines vertical with Nitrogen atom above two layers of Cu (111) surface, showing changes in adsorption orientation during MD simulation

Figure [5.7] reveals that during the MD simulation, the L-glutamines “lie down” as in the single molecule case. The molecules need only ~1 psec to change their vertical orientation and “lie down” the surface.

It should be noted that in all these cases, the L-glutamine molecules moved towards the surface with their heteroatoms Nitrogen and Oxygen. The alkyl chain moved outward the surface. This leads to the conclusion that the L-glutamine can adsorb on the surface via its functional groups (N, O) something that is in agreement with the literature [26], [20].

6. CONCLUSIONS

The adsorption behavior of L-glutamine on Cu (111) surface was investigated and its ability to act as a corrosion inhibitor by calculating the system's structural and electronic properties.

Density Functional Theory (DFT) calculations were performed by means of the SIESTA code. The clean L-glutamine shows similar structural properties with other theoretical studies. For the adsorption of L-glutamine on Cu(111) several L-glutamine's configurations (parallel or vertical to the surface) were considered and the energy minimization calculations revealed the energetically favored configuration was found to be the "On top" (showing the Nitrogen and Oxygen atoms on top of Copper atoms) along the Cu (111) surface's [110] direction. The parallel preferred orientation is in line with the L-glutamine's adsorption on Fe surfaces.

The electronic total and projected density of states retain the general features of the pure components showing an enhanced broad Cu pick form from -1 eV to -9eV while the major molecule-metal hybridizations were found around the energy range from -3 eV up to -12 eV. These results are depicted in the corresponding wavefunctions where L-glutamine's Nitrogen and Oxygen atoms form bonded states with the Cu atoms indicating their enhanced interaction. Interestingly, the HOMO state is characterized by weak hybridizations between the L-glutamine's Hydrogen atoms and the metallic surface while the LUMO reveals antibonding states.

In order to investigate the type of L-glutamine's coating on Cu (111), two molecules that cover the surface area were consider. Using energy minimization, the parallel alignment of L-glutamines was found to be energetically favoured against the anti-parallel configuration. The structural and electronic properties of the coating are similar to the single adsorbed molecule. In addition, the HOMO wavefunctions reveal hydrogen bonds between the L-glutamines and Cu (111) surface while antibonding states are found in the LUMO state. Bonding hybridizations between L-glutamines' Nitrogen and Oxygen atoms were observed at the energy range -3 eV to -5 eV while interestingly molecule-molecule intermolecular bonds were found around -3 eV to -7 eV.

These observations indicate that continues organic coating can be succeeded on Cu (111) surface due to the preference of the molecule to lie parallel to the surface and form intermolecular bonds. For this reason ab initio Molecular Dynamics (MD) simulations were performed by means of the SIESTA program. Several configurations were studied revealing interesting results. The MD simulations are in line with the energy minimization results for the on top and parallel alignment of L-glutamine on Cu (111) surface as its orientation did not changed for 2 psec close to room temperature. Interestingly the vertical L-glutamine's adsorption on the surface required only 1 psec at room temperature to rotate and lie toward the surface with its Nitrogen and Oxygen heteroatoms establishing the parallel coating on the surface.

These results could be used for the creation of metallic coatings with enhanced corrosion resistance for many applications.

7. FUTURE WORK

The results presented here have demonstrated the adsorption behavior of L-glutamine on Cu (111) surface. Furthermore other metallic surfaces like the iron ones are widely used in industry due to their enhanced magnetic properties and their protection from corrosion would be very important. For this reason adsorption of organic inhibitors on Fe or Fe/Cu surfaces could be interesting for further study. Therefore, we intent to extend this thesis and study the structural electronic and magnetic properties of the L-glutamine on copper alloys' surfaces starting from the Fe/Cu (111) surface.

8. REFERENCIES

[1]K.F. Khaled, Electrochimica Acta 53 (2008) 3484-3492

[2]Camila G. Dariva, Alexandre F. Galio . Corrosion Inhibitors- Principles, Mechanisms and Applications

[3]Mwaddam M. Kabanda, Ime B. Obot, Eno E. Ebenso,Int. J. Electrochem. Sci., 8 (2013) 10839- 10850

[4]A.Zarrouk, H. Zarrok., R.Salghi, B.Hammouti, S.S. Al-Deyab, R. Touzani, M. Bouachrine, I. Warrad, T.B. Hadda, Int. J. Electrochem. Sci., 7 (2012) 6353 – 6364

[5]Jia-jun Fu,Su-ning Li, Ying Wang Lin-hua Cao,Lu-de Lu, J Mater Sci (2010) 45:6255–6265

[6]Oguike R.S., Oni O. Int. J. Res. Chem. Environ. Vol. 4 Issue 3 (177-186) July 2014

[7]R.T. Loto, C.A. Loto, A.P.I. ,A Review. J. Mater. Sci. 3 (5) (2012) 885-894

[8]Nnabuk O. Eddy, Journal of advanced Research (2011) 2, 35-47

[9]E. M. Sherifa and Su-Moon Park, Journal of The Electrochemical Society, 152 (10) B428-B433 (2005)

[10] INGRID MILOŠEV, JASMINKA PAVLINAC, MILAN HODOŠČEK, ANTONIJA LESAR, J. Serb. Chem. Soc. 78 (12) 2069–2086 (2013)

[11]K.F. Khaled, Corrosion Science 52 (2010) 3225-3234

[12]Ambrish Singh, Eno E. Ebenso, *Int. J. Electrochem. Sci.*, 8 **(2013)** 12874 – 12883

[13] K.F. Khaled and A.M. El-Sherik, Int. J. Electrochem. Sci., 8 (2013) 10022 – 10043

[14]A. Yurt, G. Bereket, C. Ogˇretir,J. Mol. Struct. (THEOCHEM) 725 (2005) 215–221.

[15] Gokhan G., Semra Bilgic, Corrosion Sci. 52 (2010) 3435–3443

[16] Da-Quan Zhang, Bin Xie, Li-Xin Gao, Qi-Rui Cai, Hyung Goun Joo, Kang Yong Lee, Thin Solid Films 520 (2011) 356–361

[17] S. Zor, F. Kandemirli, and M. Bingul, ISSN 2070-2051, Protection of Metals and Physical Chemistry of Surfaces, 2009, Vol. 45, No. 1, pp. 46–5

[18] http://www.chemguide.co.uk/organicprops/aminoacids/background.html

[19] http://www.fao.org/docrep/W0073E/w0073e04.htm#P1625_217364

[20] ZHE ZHANG, SHENHAO CHEN, YUANYUAN FENG, YUNQIAO DING, JUANJUAN ZHOU, HENGLEI JIA, Journal of Serb. Chem. Soc. 74 (4) 407–415 (2009)

[21] International Scholarly Research Network ISRN Materials Science Volume 2012, Article ID 623754

[22] A.Zarrouk, H. Zarrok, R. Salghi, B. Hammouti, S.S. Al-Deyab, R. Touzani, M. Bouachrine, I. Warad, T. B. Hadda, Int. J. Electrochem. *Sci.,* 7 **(2012)** 6353 – 6364

[23] B. E. Amitha Rani and Bharathi Bai J. Basu Hindawi,Int. Journal of Corrosion,2012, Article ID 380217

[24] Adrian T. Murdock, Antal Koos, T. Ben Britton, Lothar Houben, Tim Batten, Tong Zhang,Angus J. Wilkinson, Rafal E. Dunin-Borkowski, Christina E. Lekka, and Nicole Grobert, ACS Nano, (2013), 7 (2), 1351–1359

[25] N. H. Rhys, A. K. Soper, and L. Dougan, J. Phys. Chem. B (2012), 116, 13308-13319

[26] Shuwei Xia, Meng Qiu, Liangmin Yu, Fuguo Liu, Haizhou Zhao, Corrosion Science 50 (2008) 2021-2029

[27] Emenka E. Oguzie, Ying Li, Sheng G. Wang and Fuhui Wang, RSC Advances, 2011, 1, 866-873

[28] http://www.chem.wisc.edu/deptfiles/genchem/sstutorial/Text7/Tx73/tx73.html

[29]http://pubchem.ncbi.nlm.nih.gov/vw3d/vw3d.cgi?cmd=crtvw&reqid=1226568992220152473#

[30] http://www.nature.com/nmat/journal/v3/n9/images/nmat1191-f4.gif

[31] Zhao Xue-Ying, Wang Hao, Yan Hao, Gai Zheng, Zhao Ru-Guang and Yang Wei-Sheng, Chin. Phys. Soc. and IOP Publishing Ltd, 2001, vol. 10, 1009-1963

[32]http://pubchem.ncbi.nlm.nih.gov/compound/L-glutamine#section=Names-and-Identifiers

[33]http://www.nual.com/NR/rdonlyres/E5F38E54-48BF-43C1-9415-865B903605EE/0/CorrosionofMetalsinElectricalApplications.pdf

[34] http://www.chemicalbook.com/ChemicalProductProperty_EN_CB6280105.htm

[35] http://www.matweb.com/reference/copper-alloys.aspx

[36] A. Bachmaier, M. Kerber, D. Setman, and R. Pippan, Acta Mater. 2012 Feb; 60(3): 860–871

[37] X.W. Wang, Surface Science 322 (1995) 51-57

[38] http://www.azom.com/article.aspx?ArticleID=7853

[39] N. M. Harrison, An Introduction to Density Functional Theory, Department of Chemistry, Imperial College of Science Technology and Medicine, SW7 2AY, London and CLRC, Daresbury Laboratory, Daresbury, Warrington, WA4 4AD

[40] Juan Carlos Cuevas, Introduction to Density Functional Theory, Institut fur Theoretische Festkorperphysik Universitat Karlsruhe (Germany)

[41] http://departments.icmab.es/leem/siesta/

[42] A. Pawlukojc´, K. Hołderna-Natkaniec, G. Bator, I. Natkaniec, Chemical Physics 443 (2014) 17–25